

Immersed figure-8 annuli and anyons

Bowen Shi

Department of Physics, University of California at San Diego, La Jolla, CA 92093, USA

March 1, 2024

Abstract

Immersion (i.e., local embedding) is relevant to the physics of topologically ordered phases through entanglement bootstrap. An annulus can immerse in a disk or a sphere as a “figure-8”, which cannot be smoothly deformed to an embedded annulus. We investigate a simple problem: is there an Abelian state on the immersed figure-8 annulus, locally indistinguishable from the ground state of the background physical system? We show that if the answer is affirmative, a strong sense of isomorphism must hold: two homeomorphic immersed regions must have isomorphic information convex sets, even if they cannot smoothly deform to each other on the background physical system. We explain why to care about strong isomorphism in physical systems with anyons and give proof in the context of Abelian anyon theory. We further discuss a connection between immersed annuli and anyon transportation in the presence of topological defects. In appendices, we discuss related problems in broader contexts.

1 Introduction

It is fascinating that many universal properties of a many-body system, such as topologically ordered phases, symmetry-protected phases, and quantum critical points, can be extracted from a single wave function [1, 2, 3, 4, 5, 6, 7, 8, 9, 10, 11]. A further surprise is that in recent years, we have seen a hope to derive [12, 13] the rules that govern those emergent theories from conditions on a state; entanglement bootstrap [14, 15, 16, 17] is a framework that aims to do this. In entanglement bootstrap, we start with a single wave function (or reference state) on a topologically trivial region, e.g., a ball or a sphere. We impose some conditions on the wave function as the starting point and derive (bootstrap) laws of the emergent theory from there. On the way to deriving the emergent physical laws, we identify information-theoretic concepts (forms of many-body entanglement), such as information convex sets and the modular commutator. The goal of entanglement bootstrap has similarities and distinctions with quantum field theory, bootstrap in other physical contexts, renormalization group, categorical theory, and solvable models. Some of these aspects have been discussed in recent works on this subject.

In this work, we investigate a simple aspect of entanglement bootstrap, the role of immersion. As we shall explain, immersion, i.e., local embedding of a topological space to another, is natural from the internal theoretical structure of the entanglement bootstrap. (Here, we are mainly interested in the case that a topological space is immersed in a background of the same space dimension. See the immersed “figure-8” annulus in Fig. 1 for an example.) The importance of immersion is noticed only gradually: see [17] for a state-of-the-art discussion and [18] for an early application with the terminology “immersion” unnoticed. We suspect that the full extent of the benefits we can reap from immersion remains largely hidden beneath the surface.

To motivate the usage of immersed regions, let us first recall why embedded regions are of interest in the study of topologically ordered systems with emergent anyonic excitations. On closed manifolds, such as tori, there can be multiple locally indistinguishable ground states. The information that distinguishes those ground states cannot be seen on any ball-shaped subsystem. Meaningful

differences can, nevertheless, be detected if we examine subsystems with nontrivial topologies, such as annuli and (punctured) tori.

In entanglement bootstrap, this intuition is made precise with the concept “information convex set” $\Sigma(\Omega)$. It is a set of density matrices on Ω , locally indistinguishable from the reference state. Originally, Ω is considered to be a subsystem, i.e., a region embedded in the physical system of interest. Smooth deformations of Ω must preserve the structure of information convex sets, according to the isomorphism theorem [14]. Thus, only the “topology class” of Ω is of interest.

Immersed regions are a broader class of regions. They are locally embedded but need not be globally embedded. Because of this, states in immersed regions can use multiple copies of local Hilbert spaces of the original physical system. For instance, states on the figure-8 annulus in Fig. 1 use the Hilbert space of the overlapping region (the region covered by two sheets) twice. Local embedding is sufficient for an information convex set to be defined [16] because we only needed local consistency of state in the information convex set with the reference state. Similarly, information convex sets are shown to be isomorphic under smooth deformation of the immersed region. To our knowledge, the topological notion of immersion rarely appeared in physics before. A notable exception is a sequence of connections observed by Hastings [19] and with Freedman [20] on invertible phases and the classification of quantum cellular automata.

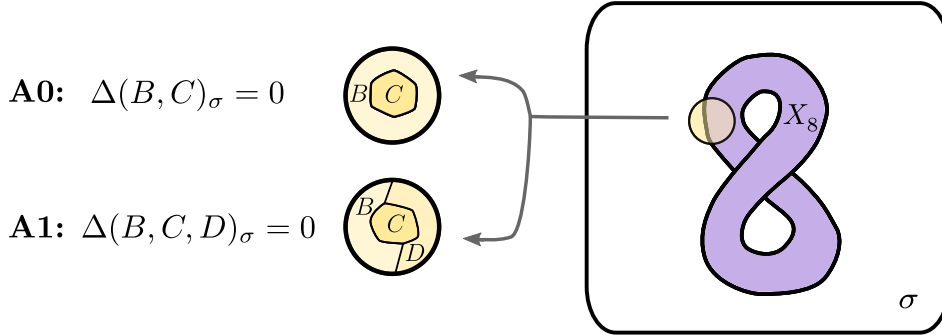


Figure 1: An immersed “figure-8” annulus (X_8) on a background 2-dimensional physical system on which we have a reference state σ . The background is often taken to be a ball or a sphere. Entanglement bootstrap axioms **A0** and **A1** are imposed on bounded radius balls such as the ball (yellow) illustrated. Entropy combinations $\Delta(B, C)$ and $\Delta(B, C, D)$ are defined in Eq. (1).

What insight can we gain by considering immersed regions? One powerful application, in entanglement bootstrap of arbitrary dimensions, is the ability to construct very rich types of immersed punctured manifolds in an n -dimensional sphere [17]. For instance, a punctured torus cannot be embedded in a 2-sphere, but it can be immersed in it. With the trick of healing the puncture, we obtain states on diverse types of closed manifolds, knowing only a state on a ball or a sphere! The ability to construct states on closed manifolds from immersion secretly agrees with that of a non-immersion approach mentioned by Kitaev in the context of invertible phases.¹

Despite the progress mentioned above, the study of immersed regions in entanglement bootstrap is still in its early stages. Some topological manifolds can immerse in topologically distinct ways, even in a sphere. A simple example is the immersed “figure-8” annulus, which cannot be smoothly deformed to an embedded annulus. One natural question is whether two homeomorphic regions Ω, Ω' immersed in the n -dimensional sphere in inequivalent classes, still have isomorphic information convex sets (Conjecture 6 and 14), which we call the strong isomorphism conjecture. One may also wonder if smooth deformation (and also “tunneling” Sec. 3.1) between different immersed regions can give interesting automorphism of information convex sets. These two problems are closely related, as we shall explain, and both are open problems.

¹See [21] at around 1 hour and 35 minutes, where the class of manifolds is referred to as normally framed manifolds.

In the main body of this work, we shall focus on the simplest 2-dimensional (2D) context. The setup of the problem is recalled in Sec. 2. We note that figure-8 X_8 represents the only nontrivial class of immersed annulus on a sphere (Table 1). We explain that the strong isomorphism conjecture for 2D boils down to a simple question about the figure-8 annulus: “is there an Abelian extreme point in $\Sigma(X_8)$?” See Sec. 3, where the intuition is that an Abelian sector on figure-8 implies that tunneling a figure-8 (Sec. 3.1) not only changes the immersion class but also acts as an isomorphism between information convex sets. Such tunneling operations are powerful enough to relate homeomorphic immersed surfaces in different classes.

Is it true that the figure-8 annulus always detects an Abelian sector? This problem appears to be nontrivial, and we provide a full solution only for Abelian anyon theories (Sec. 4), i.e., when all the anyon types detected by the embedded annulus are Abelian. The more general case is left as a conjecture.

A crucial intuition we used in the proof is that anyons transported along the figure-8 annulus cannot be permuted. We discuss a thought experiment “transportation experiment” (Sec. 5), that broadens the scope of this idea and applies it to physical contexts with topological defects. It relates the property of immersed annulus that thickens the transportation loop to the question of if anyons are permuted after the transportation. Many ideas and questions generalize to higher dimensions. In the appendix, we discuss a few tools useful in thinking about such generalizations.

2 Background

This section is a review of some necessary background information for entanglement bootstrap. We shall focus on the concept of immersed regions and related facts. In particular, we explain why there are precisely two classes of immersed annuli in a sphere; see Table 1.

2.1 Setup and axioms

We consider entanglement bootstrap setup in two spatial dimensions (2D). We consider a reference state σ on a 2D surface. Unless stated otherwise, we consider a reference state on the sphere \mathbf{S}^2 . (We used bold font to emphasize that a reference state is defined on the sphere.) In this case, $\sigma = |\psi\rangle\langle\psi|$.² We assume that the total Hilbert space is a tensor product of on-site Hilbert spaces from sites (or cells) of a coarse-grained lattice. The local Hilbert space for each coarse-grained site is finite-dimensional.

The axioms **A0** and **A1** are imposed on small balls containing a few coarse-grained lattice sites. The regions are described in Fig. 1, where

$$\Delta(B, C, D) \equiv S_{BC} + S_{CD} - S_B - S_D, \quad \text{and} \quad \Delta(B, C) \equiv \Delta(B, C, \emptyset). \quad (1)$$

Here $S_A|_\rho$ means $S(\rho_A) = -\text{Tr}(\rho_A \ln \rho_A)$ is the von Neumann entropy. The strong subadditivity [22] implies useful inequalities of similar (but diverse) forms. A particularly useful one to keep in mind is that, for any ρ_{ABCD} , $\Delta(B, C, D)_\rho \geq I(A : C|B)_\rho \geq 0$. Here $I(A : C|B) \equiv S_{AB} + S_{BC} - S_B - S_{ABC}$ is the conditional mutual information.

Remark. The axioms **A0** and **A1** stated that the entropy conditions hold precisely. This can be a pretty strong requirement even though whole classes of solvable models satisfy these conditions precisely [23]. Nevertheless, there is evidence that precisely satisfied axioms are too strong to accommodate chiral topological orders.³ From the physical standing point, the right way to appreciate

²Starting with a ball or a sphere is equivalent due to the “completion trick” [16]. We shall take \mathbf{S}^2 to be explicit. The important thing is that we do not need a state on a topologically nontrivial manifold.

³At least, this should be true if the local Hilbert space on each site is finite-dimensional. One piece of evidence comes from an unpublished work with Daniel Ranard, Ting-Chun Lin, and Isaac Kim, where a commuting projector parent Hamiltonian is identified.

these axioms is that we expect them to hold more accurately in larger systems. The first appearance of entropy in physics is in thermodynamics, where the prediction works best for large systems. We draw the parallel and argue that entanglement bootstrap predictions are also relevant for systems with approximate axioms. In fact, for chiral phases, a certain formula initially argued used precise area law [8] found confirmation with another theoretical approach [24] in the range of validity of the latter.

The axioms are imposed on an intermediate length scale, which is much smaller than the total system size and larger than the correlation length and (microscopic) lattice spacing. This can be viewed as one instance of starting from the “middle” [25] rather than the “bottom” [26], where entanglement bootstrap may be considered as one of those most quantum cases. Indeed, suppose the two axioms are satisfied on some intermediate scale. In that case, the same conditions hold on all larger length scales, and they define a renormalization group fixed point in this sense.

Remark. It is a conjecture that if the violations of the axioms are small enough, coarse-grain the lattice further will result in more accurate axioms. These are “threshold conjectures”; see Chapter 11 of [27] for a version and an explanation of why a threshold $0 < \delta < \ln 2$ of violation of **A1** is consistent with current examples from spurious topological entanglement entropy, non-Abelian anyons, domain walls, and defects.

Although we are mainly interested in systems where the axioms hold, some concepts and insights developed in entanglement bootstrap, such as the idea of considering quantum states on immersed regions, may be useful in broader contexts as well.

2.2 Immersed annuli and its classification

Immersed regions are locally embedded regions. For each immersed region, an information convex set can be defined [14, 16]. An information convex set is a set of density matrices on a region Ω that can locally extend and are locally identical to the reference state σ . Any locally embedded region has a “good enough” set of balls to check such consistency conditions, and thus, an information convex set $\Sigma(\Omega)$ is defined. Embedded regions, also called “subsystems,” are special cases of immersed regions. (We shall denote “ Ω is immersed in Y ” by $\Omega \looparrowright Y$.)

The isomorphism theorem says if two immersed regions $(\Omega, \Omega' \looparrowright \mathbf{S}^2)$ can be smoothly⁴ deformed to each other, the information convex sets associated with them are isomorphic. We denote this as

$$\Omega \stackrel{\mathbf{S}^2}{\sim} \Omega' \quad \Rightarrow \quad \Sigma(\Omega) \cong \Sigma(\Omega'). \quad (2)$$

By isomorphism “ \cong ”, we mean the existence of an invertible map $\Phi : \Sigma(\Omega) \rightarrow \Sigma(\Omega')$ that preserves both the entropy difference and the fidelity between any pair of elements. Generally, for two immersed regions $\Omega, \Omega' \looparrowright Y$, we say $\Omega \stackrel{Y}{\sim} \Omega'$ if two regions can be smoothly deformed to each other on Y .⁵

Below, we shall be interested in immersed annuli. As the isomorphism theorem implies, only the topological class is of interest. We explain below that there are only two topological classes of immersed annuli, denoted by X and X_8 ; see Table 1. (We adopt two alternative ways to draw X_8 . One is as in Fig. 1, where the overlap part is shown as two layers, one on top and it covers another layer. The second way is as Table 1, where the overlap part is transparent so that we see both layers. We note that the “top and bottom” in the first way is introduced for drawing purposes only,

⁴In entanglement bootstrap, we have a coarse-grained lattice rather than a smooth manifold, in which context “smooth deformation” always means applying elementary steps; see Section 3.3 of [14].

⁵An alternative way to say two regions can be deformed to one another smoothly through immersed configurations is to say there is a regular homotopy, a term adopted from differential topology. More precisely, regular homotopy is about maps, and we have modulo-out automorphisms. This convention can similarly be traced back to math literature, e.g. “immersed surface” defined in [28].

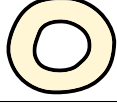
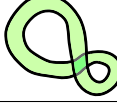
region's name	embedded annulus	figure-8
symbol	X	X_8
region		
turning number	1	0
superselection sectors	$\mathcal{C} = \{1, a, b, \dots\}$	$\mathcal{C}_8 = \{\mu, \nu, \lambda, \dots\}$

Table 1: The two topological classes of immersion of annuli in a sphere. One is represented by the embedded annulus X , and another is represented by the nontrivially immersed “figure-8” X_8 . Labels of superselection sectors, in the last line, follow from the simplex theorem reviewed in Section 2.3.

and this is not part of the data to specify immersion. We shall frequently use the first approach as it simplifies drawing.) We shall be interested in knowing if $\Sigma(X) \cong \Sigma(X_8)$, which is not answered by the isomorphism theorem.

According to Table 1, figure-8 X_8 is the only nontrivial immersion type on a sphere. This fact follows from the following argument. First, on the disk (B^2), each immersed annulus is the thickening of some curve in B^2 , where the curve has no sharp corners. Therefore, they are classified by the turning number (modulo the sign). Two regions with different turning numbers cannot be converted to each other, as is well-known [29]. Some allowed and not allowed deformations on B^2 are illustrated as follows:

$$\bigcirc \stackrel{B^2}{\sim} \bigcirc \quad \bigcirc \stackrel{B^2}{\not\sim} \bigcirc \quad \bigcirc \stackrel{B^2}{\not\sim} \bigcirc \quad \bigcirc \stackrel{B^2}{\sim} \bigcirc \quad \bigcirc \stackrel{B^2}{\not\sim} \bigcirc \quad (3)$$

Here, each thick curve represents an immersed annulus, $\stackrel{B^2}{\sim}$ means two immersed regions can be smoothly deformed to each other on the background B^2 , whereas $\not\sim$ means impossible to do such deformation. On the sphere, there is an extra deformation that lets the annulus sweep over the entire sphere! This process can change the turning number by an even integer and thus further reduces the classification:

$$\bigcirc \stackrel{S^2}{\sim} \bigcirc \quad \bigcirc \stackrel{S^2}{\sim} \bigcirc \quad \bigcirc \stackrel{S^2}{\not\sim} \bigcirc \quad (4)$$

Consequently, we end up with two equivalence classes of immersed annuli. These two classes are represented by the embedded annulus X and the immersed figure-8 annulus X_8 , as described in Table 1.

The central nontrivial claim of the isomorphism theorem is the *existence* and uniqueness of a density matrix on another region that shares some property of an existing density matrix. This comes from a powerful “merging technique”, which enters the proof of the isomorphism theorem. The merging technique works even if we modify the topology of the region. In a later section, we shall review the merging technique when we use it in important ways.

2.3 Superselection sectors and fusion spaces

Information convex sets detect superselection sectors and fusion spaces. In 2D, an embedded annulus X detects the anyon types $\mathcal{C} = \{1, a, b, \dots\}$, and here 1 denotes the vacuum sector. The 2-hole disk (Fig. 2 (a)) detects the fusion spaces. These follow from the structure theorems: simplex theorem and Hilbert space theorem in the original paper [14]. The simplex theorem states that the

information convex set of the embedded annulus, $\Sigma(X)$, is a simplex:

$$\Sigma(X) = \left\{ \rho_X \left| \rho_X = \sum_{a \in \mathcal{C}} p_a \rho_X^a \right. \right\}, \quad (5)$$

where the extreme points ρ_X^a (which are density matrices⁶) are mutually orthogonal, that is, the fidelity between ρ_X^a and ρ_X^b is zero when $a \neq b$. $\{p_a\}$ is a probability distribution, and the set of extreme point labels $\mathcal{C} = \{1, a, b, \dots\}$ is finite.

Remark. More generally, the simplex theorem works for any sectorizable region [15]. Sectorizable is a topological condition that says S contains disjoint subsets S_1 and S_2 , each of which can deform back to S by a sequence of elementary extensions. In 2D, immersed annuli and disks are the only sectorizable regions. A Möbius strip embedded in RP^2 is not sectorizable, even though it is the thickening of some loop.

Of importance is the fact that the simplex theorem works equally well for immersed regions, e.g., figure-8 X_8 . The vacuum state is, however, defined *only* for embedded annulus:

- $\mathcal{C} = \{1, a, b, \dots\}$ is the superselection sectors defined from embedded annulus X . The vacuum “1” is associated with a special extreme point, the reference state $\rho_X^1 \equiv \sigma_X$.
- $\mathcal{C}_8 = \{\mu, \nu, \lambda, \dots\}$ is the set of superselection sectors defined from the figure-8 X_8 . We do not assume the existence of a vacuum.⁷

Here are a few words about antiparticles. \mathcal{C} has a natural notion of antiparticle, that is, for each $a \in \mathcal{C}$, there is a unique $\bar{a} \in \mathcal{C}$ such that $a \times \bar{a} = 1 + \dots$; one way to define antiparticle is to deform the annulus X back to itself in a nontrivial way on the sphere. It is a further interesting question on whether \mathcal{C}_8 has a natural definition of antiparticle, too. It seems natural to consider the following automorphism of $\Sigma(X_8)$:



$$(6)$$

A more careful (and broader) discussion is postponed in Appendix B.

A general immersed region (Y) can detect a fusion space $\mathbb{V}_I(Y)$. Let ∂Y be the thickened boundary⁸ of Y . In general, ∂Y can have multiple connected components, and each component is an annulus, either an embedded annulus (like X) or a nontrivially immersed annulus (like X_8). The label I is then a collection of ordered labels from \mathcal{C} and \mathcal{C}_8 . Two instances are shown in Fig. 2, where $I = (a, b, c)$ for Fig. 2(a) and $I = (\mu, a, \nu)$ for Fig. 2(b). Once we specify the label I , we get a convex subset $\Sigma_I(Y)$ isomorphic to the state space (i.e., the space of density matrices) of a finite-dimensional fusion space \mathbb{V}_I :

$$\Sigma_I(Y) \cong \mathcal{S}(\mathbb{V}_I). \quad (7)$$

This is the main content of the Hilbert space theorem. Furthermore, the thickened boundary ∂Y is sectorizable, and it is useful to denote the set of superselection sectors as $\mathcal{C}_{\partial Y}$ and note $I \in \mathcal{C}_{\partial Y}$.

⁶These extreme points are, in general, mixed states.

⁷The existence of the vacuum state for the figure-8 may be a logical consequence of the axioms. This remains an open problem.

⁸In entanglement bootstrap, a thickened (entanglement) boundary $\partial\Omega$ of a region Ω , ($\partial\Omega \subset \Omega$), is the region Ω with its interior removed.

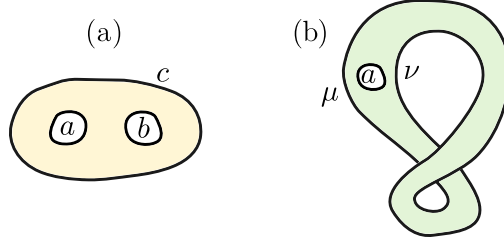


Figure 2: Examples of regions that detect fusion spaces. (a) A region that detects \mathbb{V}_{ab}^c , and (b) a region that detects $\mathbb{V}_{\mu a}^\nu$. Here, $a, b, c \in \mathcal{C}$ and $\mu, \nu \in \mathcal{C}_8$.

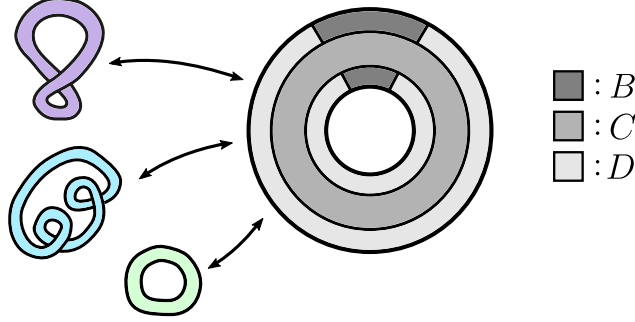


Figure 3: The partition of an immersed annulus $Z = BCD$ used in defining quantum dimension (Definition 1). We first map the immersed annulus to a topological annulus by some homeomorphism indicated by the arrow. We then partition the topological annulus as illustrated.

2.4 Quantum dimensions

We give a definition of quantum dimension for superselection sectors detected by immersed annuli. (A generalization into arbitrary spatial dimensions is presented in Appendix A.) Formally, the definition is as follows:

Definition 1 (Quantum dimension). Let Z be an immersed annulus. Let $Z = BCD$, where $BD = \partial Z$ is the thickened boundary and $C = Z \setminus \partial Z$ is the interior; B and D each is a union of two disks, as illustrated in Fig. 3. For any extreme point $\rho_Z^h \in \Sigma(Z)$,

$$d_h \equiv \exp \left(\frac{\Delta(B, C, D)_{\rho^h}}{4} \right) \quad (8)$$

is the quantum dimension of the superselection sector h .

Immediately following this definition, we have

1. $d_h \geq 1$ for any $h \in \mathcal{C}_Z$, where \mathcal{C}_Z is the set of superselection sectors characterized by $\Sigma(Z)$. This follows immediately from strong subadditivity $\Delta(B, C, D) \geq 0$. Note that $\mathcal{C}_Z = \mathcal{C}$ if $Z \stackrel{\mathbb{S}^2}{\sim} X$ and $\mathcal{C}_Z = \mathcal{C}_8$ if $Z \stackrel{\mathbb{S}^2}{\sim} X_8$.
2. Importantly, Definition 1 does not require the knowledge (or existence) of a vacuum state on Z . On the other hand, for the embedded annulus X , where the vacuum is defined, Definition 1 is equivalent to another definition $d_a \equiv \exp \left(\frac{S(\rho_X^a) - S(\rho_X^1)}{2} \right)$.
3. Definition 1 works even if we relax the topology of the region that defines the reference state. This general setup allows topological defects and is relevant to some discussion later in Section 5 and in Appendix B.

Definition 2 (Abelian sector). A superselection sector h of an immersed annulus is Abelian if d_h in Definition 1 gives $d_h = 1$.

Definition 3 (Abelian anyon theory). In the context of entanglement bootstrap in 2D, we say the theory is Abelian if $d_a = 1, \forall a \in \mathcal{C}$.

Note that the definition of Abelian anyon theory only puts a requirement on the embedded annulus. For various reasons, we will need the following lemma.

Lemma 4 (Abelian sector criterion). *Let $\rho_Z \in \Sigma(Z)$, where Z is an immersed annulus, the following are equivalent:*

0. ρ_Z is an extreme point of $\Sigma(Z)$ associated with an Abelian sector.
1. $\Delta(B, C, D)_\rho = 0$ for the partition in Fig. 3.
2. $\Delta(B, C, D)_\rho = 0$ for the partition in Fig. 4(a).
3. $\Delta(B, C, D)_\rho = 0$ for the partition in Fig. 4(b).
4. $I(A : C|B)_\rho = 0$ for the partition in Fig. 4(c).

According to Lemma 4, any one of the conditions 1, 2, 3, and 4 can be used to determine if a state in $\Sigma(Z)$ is an extreme point associated with Abelian superselection sector.

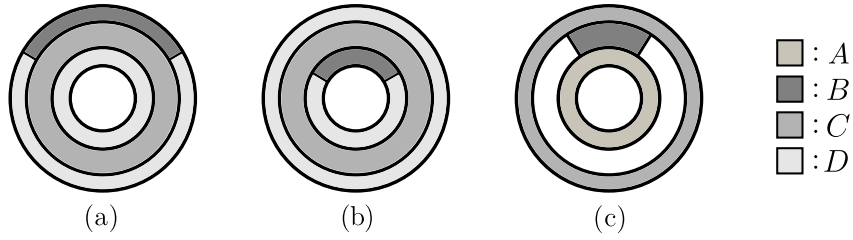


Figure 4: As with Fig. 3, we mapped the immersed annulus to the topological annulus by some (fixed) homeomorphism. Three distinct partitions of the annulus are shown in (a), (b), and (c).

Proof. First, suppose that ρ_Z is an extreme point of $\Sigma(Z)$. According to the definition of quantum dimension, $\Delta(B, C, D)_\rho = 0$ for the partition in Fig. 3. It follows from Lemma 12 in Appendix A that any one of conditions 1, 2, 3, 4 implies the rest of them. (Lemma 12 in the appendix is a more general statement about the equivalence of definitions for quantum dimension, works beyond 2D setups.) Second, none of 1, 2, 3, 4 is true if $\rho_Z = \sum_h p_h \rho_Z^h$ is a non-extreme point. This is because a non-extreme point has contribution $\sum_h p_h \ln\left(\frac{1}{p_h}\right) > 0$ added to Δ s and I in conditions 1, 2, 3, 4. This contribution is always positive for non-extreme points. These two considerations derive Lemma 4. \square

3 Fun with figure-8

We have learned that the “figure-8” region X_8 represents the only nontrivial class of immersed annulus in the sphere (Table 1). It is arguably the simplest nontrivial immersed region and is fun to play with. The set of superselection sectors detected by X_8 are $\mathcal{C}_8 = \{\mu, \nu, \dots\}$. Throughout this section, we assume a reference state $\sigma = |\psi\rangle\langle\psi|$ on a sphere \mathbf{S}^2 , and the axioms **A0** and **A1** are satisfied everywhere on the reference state. Also, recall that X represents the embedded annulus, which can detect the anyon types $\mathcal{C} = \{1, a, b, \dots\}$.

The seemingly simple figure-8 region (X_8) already has interesting puzzles. The simplest one is on the existence of an Abelian sector in \mathcal{C}_8 :

Conjecture 5 (Abelian sector on figure-8). $\exists \mu \in \mathcal{C}_8$, such that $d_\mu = 1$.

We emphasize that the conjecture is made in the context where the reference state is defined on sphere \mathbf{S}^2 . An alternative version of the conjecture requires the reference state σ defined on a disk. These two versions are equivalent due to the ability to “complete” the disk into a sphere. One may wonder if it is possible to relax the support of the reference state further. This is impossible. If the reference state is defined on an annulus, there may not be an Abelian sector, even for an embedded annulus; this is due to topological defects, see Section 5.1. We shall prove Conjecture 5 for Abelian anyon theory in Section 4.

Another natural question about figure-8 is whether or not

$$\Sigma(X_8) \cong \Sigma(X). \quad (9)$$

The weaker statement $|\mathcal{C}_8| = |\mathcal{C}|$, i.e., the number of extreme points of $\Sigma(X_8)$ equals the number of anyon species is true; we will discuss this in Section 5. If the two information convex sets $\Sigma(X_8)$ and $\Sigma(X)$ are isomorphic in the most natural manner, we expect an invertible map between them that preserves the quantum dimensions. Then, in addition to $|\mathcal{C}| = |\mathcal{C}_8|$, we should have an Abelian sector of \mathcal{C}_8 that is mapped to the vacuum $1 \in \mathcal{C}$. This is one way to motivate Conjecture 5. (It is a further question whether there is a “canonical vacuum” on \mathcal{C}_8 .)

An intriguing and nontrivial observation, which we shall make later in this section, is that Conjecture 5 not only implies the seemingly stronger $\Sigma(X_8) \cong \Sigma(X)$ but also implies a very powerful “strong isomorphism”:

Conjecture 6 (2D strong isomorphism conjecture).

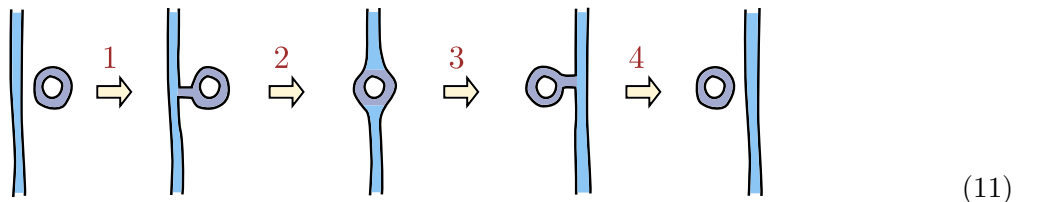
$$\Omega, \Omega' \looparrowright \mathbf{S}^2 \text{ are homeomorphic} \Rightarrow \Sigma(\Omega) \cong \Sigma(\Omega'). \quad (10)$$

Importantly, we only required that Ω and Ω' are homeomorphic, and this is strictly weaker than $\Omega \stackrel{\mathbf{S}^2}{\sim} \Omega'$. (The weaker statement: $\Omega \stackrel{\mathbf{S}^2}{\sim} \Omega'$ implies $\Sigma(\Omega) \cong \Sigma(\Omega')$ is a known fact, from isomorphism theorem.) This motivates the name “strong isomorphism conjecture”. As is evident, Eq. (9) is implied by the strong isomorphism conjecture. It is straightforward to generalize Conjecture 6 to arbitrary spatial dimensions; see Appendix C. As a reminder, \cong means there exists an isomorphism. It does not imply a “canonical” isomorphism. \cong preserves the entropy difference and fidelity between two elements.

3.1 Tunneling trick

We introduce a tunneling trick. The essential observation is that tunneling a figure-8 through a strip can add a twist to the strip. If the “figure-8” region carries an Abelian sector, this process generates an isomorphism between information convex sets associated with homeomorphic topological regions in possibly distinct regular homotopy classes. We first explain the tunneling process at a topological level. After that, we discuss the details of entanglement bootstrap and explain what tunneling does on the quantum state (density matrices) and why an Abelian sector in \mathcal{C}_8 plays a role.

At the topological level, the tunneling process contains a few steps. This is illustrated in Fig. 5. In the first step, we attach X_8 to the strip by a small disk on the right. In the second and third steps, we deform the region such that X_8 disappears from the right and appears at the left of the strip, still attached. In the fourth step, we detach X_8 . By the end of the tunneling process, a twist is added to the strip. It is instructive to compare the tunneling of X_8 with the tunneling of an embedded annulus X :



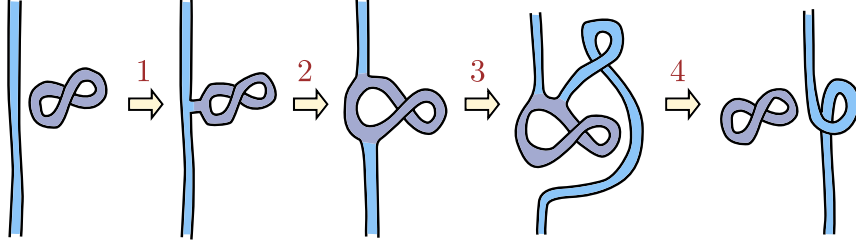


Figure 5: The topological detail of tunneling a figure-8 X_8 through a strip. The strip can be thought of as a “local piece” (in fact, a 1-handle) of some larger immersed region.

Tunneling an embedded annulus does not add any twist to the strip. The difference in the turning number between X_8 and X matters, and thus X_8 is of importance here.

What does the tunneling process in Fig. 5 mean in entanglement bootstrap? It represents a transformation of the quantum state (density matrix) on the region containing the strip. Let the region containing the original strip be A and the region containing the strip after tunneling be A' , (see Fig. 6). Suppose, the state on “figure-8” C is an extreme point ρ_C^μ , with $\mu \in \mathcal{C}_8$. The transformation, as we shall discuss, must be a quantum channel that depends on μ :

$$\Phi(\mu) : \Sigma(A) \rightarrow \Sigma(A'). \quad (12)$$

The quantum channel $\Phi(\mu)$ can be written as a product of three quantum channels

$$\Phi(\mu) = \Gamma^{\text{det}} \circ \Phi_{ABC \rightarrow A'B'C'}^{\text{deform}} \circ \Gamma^{\text{att}}, \quad (13)$$

where the attaching map $\Gamma^{\text{att}} : \Sigma(A) \rightarrow \Sigma_{[\rho_C^\mu]}(ABC)$ is a merging process, as we explain in the next paragraph. $\Sigma_{[\rho_C^\mu]}(ABC)$ is the subset of $\Sigma(ABC)$ with the constraint that the state reduces to C gives ρ_C^μ . The deformation map $\Phi_{ABC \rightarrow A'B'C'}^{\text{deform}} : \Sigma_{[\rho_C^\mu]}(ABC) \rightarrow \Sigma_{[\rho_{C'}^\mu]}(A'B'C')$ is associated with the deformation (steps 2 and 3 of Fig. 5). This channel is an isomorphism (by the isomorphism theorem). The detaching map $\Gamma^{\text{det}} : \Sigma_{[\rho_{C'}^\mu]}(A'B'C') \rightarrow \Sigma(A')$ is the partial trace $\text{Tr}_{B'C'}$. In summary, the three quantum channels are

$$\begin{aligned} \Gamma^{\text{att}} : \Sigma(A) &\rightarrow \Sigma_{[\rho_C^\mu]}(ABC), & \text{step 1 of Fig. 5} \\ \Phi_{ABC \rightarrow A'B'C'}^{\text{deform}} : \Sigma_{[\rho_C^\mu]}(ABC) &\rightarrow \Sigma_{[\rho_{C'}^\mu]}(A'B'C'), & \text{step 2 and 3 of Fig. 5} \\ \Gamma^{\text{det}} : \Sigma_{[\rho_{C'}^\mu]}(A'B'C') &\rightarrow \Sigma(A'), & \text{step 4 of Fig. 5} \end{aligned} \quad (14)$$

In fact, any one of them is a sequence of Petz maps [30] and partial traces.

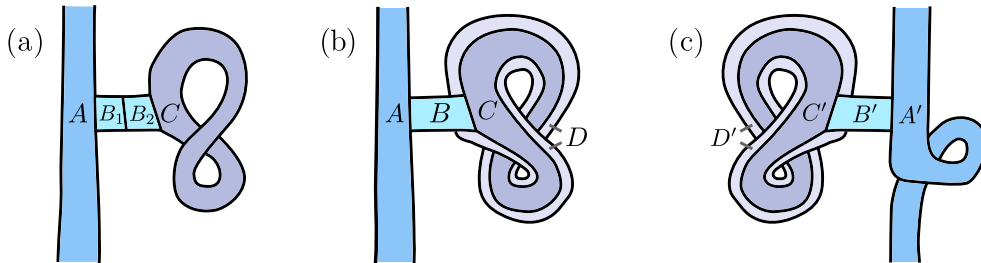


Figure 6: Analyzing the attachment (detachment) of an immersed figure-8 annulus C (C'). Only part of A , A' are shown. (a) A partition for merging. (b) and (c) have special usage when the state on “figure-8” is an Abelian extreme point.

The attachment map Γ^{att} is defined as follows. Consider an arbitrary state $\lambda_A \in \Sigma(A)$ and an arbitrary extreme point $\rho_C^\mu \in \Sigma(C)$, with $\mu \in \mathcal{C}_8$; the partitions are those in Fig. 6(a). First, we

extend λ_A to $\lambda_{AB} \in \Sigma(AB)$ and extend ρ_C^μ to $\rho_{BC}^\mu \in \Sigma(BC)$. Such an extension is unique because we enlarge the regions smoothly. $B = B_1 B_2$. The two states obey the conditions for merging:

$$I(A : B_2 | B_1)_\lambda = 0, \quad I(C : B_1 | B_2)_{\rho^\mu} = 0, \quad \text{Tr}_A \lambda_{AB} = \text{Tr}_C \rho_{BC}^\mu. \quad (15)$$

According to the merging lemma [31, 14], there is a unique state τ_{ABC} satisfying (i) τ_{ABC} reduces to λ_{AB} on AB and reduces to ρ_{BC}^μ on BC , (ii) $I(A : C | B)_\tau = 0$. Then, by the merging theorem [14, 15], the state τ_{ABC} is in the information convex set $\Sigma(ABC)$, and in fact it is in the convex subset $\Sigma_{[\rho_C^\mu]}(ABC)$. The attachment map Γ^{att} is defined such that $\tau_{ABC} = \Gamma^{\text{att}}(\lambda_A)$. Importantly, Γ^{att} is a sequence of Petz maps acting in a local neighborhood of the strip. It depends on μ through merging, and it is independent of λ_A .

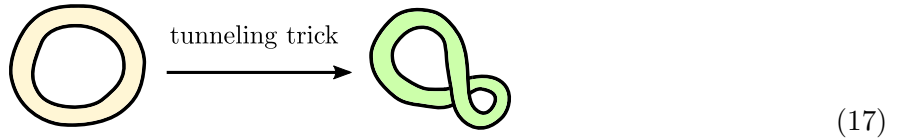
The discussion of the attachment map so far is for general $\mu \in \mathcal{C}_8$. If μ is non-Abelian, the map $\Gamma^{\text{att}} : \Sigma(A) \rightarrow \Sigma_{[\rho_C^\mu]}(ABC)$ may not be an isomorphism. (The same is true already for tunneling an embedded annulus in the context of Eq. (11).) The important thing, as we shall explain, is that if $\mu \in \mathcal{C}_8$ is Abelian, Γ^{att} and Γ^{det} are isomorphisms. The special property of Abelian sectors relevant to Γ^{att} is that for any Abelian $\mu \in \mathcal{C}_8$,

$$I(A : C | B)_\alpha = 0, \quad \forall \alpha \in \Sigma_{[\rho_C^\mu]}(ABC). \quad (16)$$

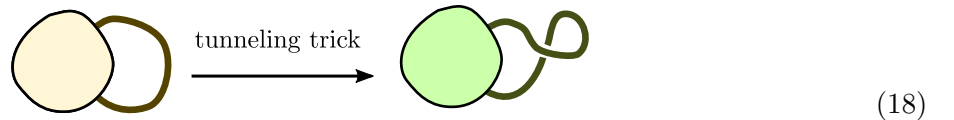
The derivation of Eq. (16) is as follows. We first extend the state $\alpha_{ABC} \in \Sigma_{[\rho_C^\mu]}(ABC)$ to a state in $\Sigma(ABCD)$, as in Fig. 6(b). If μ is Abelian, by Lemma 4, we have $\Delta(B, C, D)_{\rho^\mu} = 0$. Then by strong subadditivity, $I(A : C | B)_\alpha \leq \Delta(B, C, D)_{\rho^\mu} = 0$. Because of its quantum Markov state structure, α_{ABC} can be recovered from α_{AB} by a quantum channel independent of α_{AB} (but depend on ρ^μ). The fact that this α -independent quantum channel reverses the partial trace Tr_C implies that Γ^{att} is an isomorphism. For the same reason, the detachment map Γ^{det} is an isomorphism too. (The state exists by merging. The reversibility follows from $I(A' : C' | B') = 0$.)

In summary, tunneling a figure-8 region (Fig. 5) induces a quantum channel of the form Eq. (12). The channel $\Phi(\mu)$ is an isomorphism if $\mu \in \mathcal{C}_8$ is Abelian.

As an application, we see that $\Sigma(X_8) \cong \Sigma(X)$ if $\exists \mu \in \mathcal{C}_8$ such that $d_\mu = 1$, (that is if Conjecture 5 holds). This is because we can tunnel a figure-8 through X and turn X into a figure-8 X_8 . This result is summarized as follows:



Another way to illustrate this result uses the idea of handle decomposition; see e.g., Chapter 4 of [32]. An annulus is the union of a 0-handle with a 1-handle. The difference between the embedded annulus X and the immersed “figure-8” X_8 is the absence or existence of a twist on the 1-handle. We thus redraw (17) as:



Here, a 0-handle is a disk (the round part of the figure), and a 1-handle is the strip (thick lines in the figure). Both 0-handles and 1-handles are topological balls. The difference is the way they attach. This way of illustration will be convenient in the following.

3.2 Abelian sector on “figure-8” implies 2D strong isomorphism

Now, we are in the position to explain why if the figure-8 annulus has an Abelian sector (i.e., if Conjecture 5 is true), then the strong isomorphism conjecture (Conjecture 6) holds. This uses the tunneling trick discussed in Section 3.1. We explain why the trick is general enough.

In the remainder of the section, we assume the existence of $\mu \in \mathcal{C}_8$, such that $d_\mu = 1$. The proof of strong isomorphism of an arbitrary region reduces to the study of connected regions pretty straightforwardly. Thus, we only consider connected regions $\Omega \looparrowright \mathbf{S}^2$ below. Because Ω is connected and is immersed in \mathbf{S}^2 , it is either the sphere itself or it is an orientable surface with boundaries. Nothing needs to be proved for the case Ω is the sphere itself, and thus we consider the latter case. An orientable surface with boundaries can be written as a connected sum of $k \geq 0$ tori⁹ ($\#kT^2$) with $m \geq 1$ holes; see, e.g. [33]. Thus, such an Ω is a *boundary connected sum* of k punctured tori $T^2 \setminus B^2$ and $m - 1$ annuli.

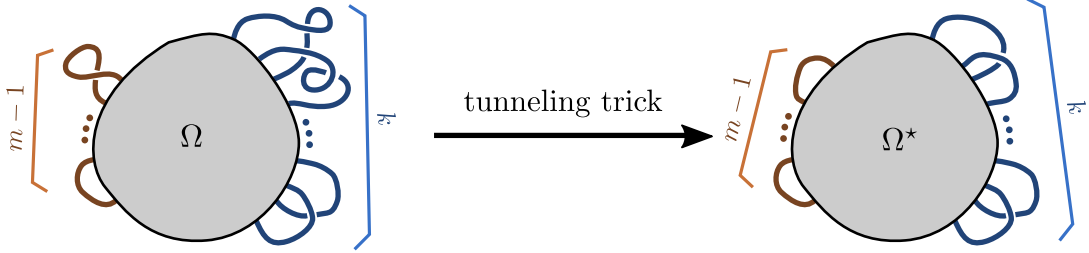


Figure 7: Tunneling trick applied to a connected region immersed in the sphere.

Objects participating in the boundary connected sum can slide around each other since they are connected by 1-handles. (Such sliding works for both embedded regions and the more general classes of immersed regions.) It follows that we can smoothly deform Ω on \mathbf{S}^2 such that it looks like the left figure of Fig. 7. It is a 0-handle with $2k + m - 1$ 1-handles attached in the order (around the 0-handle) indicated in the figure. Some of the 1-handles have twists. Upon the removal of possible twists, Ω becomes Ω^* in the right figure of Fig. 7. In Ω^* , the 1-handles form two groups: $(m - 1)$ of them are separated from others (dark brown), and there are k pairs of 1-handles (dark blue), the two 1-handles in each pair “cross” each other. Importantly, in both figures in Fig. 7, we can arrange the 1-handles in the same order, circling around the 0-handle (the chunky gray disk), thanks to the ability to slide the components around each other.

Thus, for any connected $\Omega \looparrowright \mathbf{S}^2$, we can find a “standard” immersed region $\Omega^* \looparrowright \mathbf{S}^2$ in the homeomorphism class of Ω such that we can convert Ω to Ω^* by the tunneling trick. Then, suppose there is an Abelian sector on “figure-8”, the tunneling trick implies the isomorphism

$$\Sigma(\Omega) \cong \Sigma(\Omega^*). \quad (19)$$

Then, consider another region $\Omega' \looparrowright \mathbf{S}^2$ in the homeomorphism class of Ω , we can do the same trick and show $\Sigma(\Omega') \cong \Sigma(\Omega^*)$. It follows that $\Sigma(\Omega) \cong \Sigma(\Omega')$. This completes the argument.

4 Proofs in the context of 2D Abelian anyon theory

We can derive a concrete result (Proposition 7) for Abelian anyon theories in 2D. It implies that Conjecture 5 and Conjecture 6 are true for Abelian anyon theories.

Proposition 7. *If $d_a = 1, \forall a \in \mathcal{C}$, then $d_\mu = 1, \forall \mu \in \mathcal{C}_8$.*

The proof uses Fig. 8, where the key idea is that any anyon transported along the “figure-8” does not change its type. Same with Section 3, we would like to think of the figure-8 region in Fig. 8 to be embedded in either a ball or a sphere. However, it turns out that the argument only needs a certain property of the neighborhood of the figure-8 region. This is advantageous, and the same idea works in the transportation experiment in the next section.

⁹The $k = 0$ case, in our convention, is a sphere with m holes.

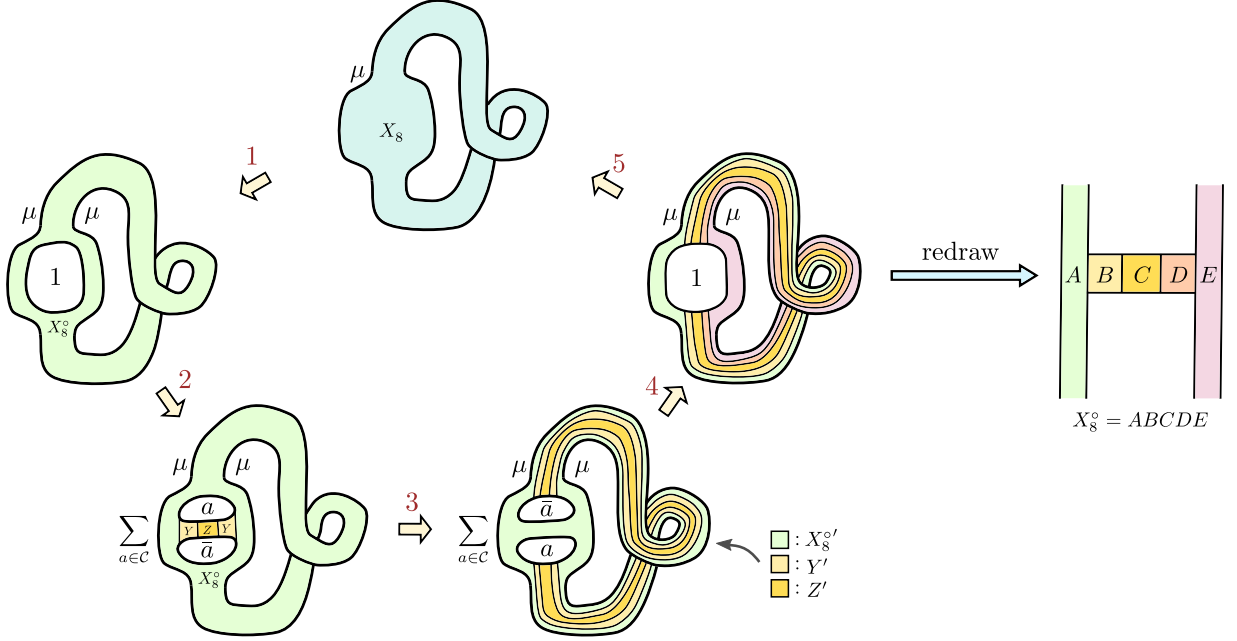


Figure 8: Operations on an extreme point $\rho_{X_8}^\mu \in \Sigma(X_8)$, where X_8 is an immersed figure-8 and $\mu \in \mathcal{C}_8$. These are useful in proving Proposition 7, where we require $d_a = 1, \forall a \in \mathcal{C}$. The end result of the analysis is a useful condition $I(A : E|BCD)_{\rho^\mu} = 0$ on the figure we redraw on the right; only part of the annuli A and E are shown.

Proof. We consider a sequence of operations applying to a state on “figure-8” X_8 carrying an arbitrary $\mu \in \mathcal{C}_8$; see Fig. 8. We denote this extreme point of $\Sigma(X_8)$ as $\rho_{X_8}^\mu$. We draw X_8 in such a way that part of the “figure-8” annulus is blown up. The region is like a “watch with a twisted belt”. We shall explain the steps in Fig. 8 and the fact that they imply a useful condition Eq. (23) on the $\rho_{X_8}^\mu$. Below are the details.

In Step 1, we take a partial trace to create a hole in the interior of X_8 . We call the resulting region X_8^o . The hole carries the vacuum sector $1 \in \mathcal{C}$. The two boundaries of the original figure-8 shape carry identical superselection sectors $\mu \in \mathcal{C}_8$. In Step 2, we merge a disk (YZ) to the hole. The resulting region $X_8^o YZ$ is in a state

$$\tilde{\rho}_{X_8^o YZ}^\mu = \frac{1}{|\mathcal{C}|} \sum_{a \in \mathcal{C}} \rho_{X_8^o YZ}^{a\bar{a}\mu\mu}, \quad I(X_8^o : Z|Y)_{\tilde{\rho}^\mu} = 0, \quad (20)$$

where the state $\tilde{\rho}_{X_8^o YZ}^\mu$ is an element in the information convex set $\Sigma(X_8^o YZ)$ and it is the indicated convex combination of extreme points $\rho_{X_8^o YZ}^{a\bar{a}\mu\mu}$ of $\Sigma(X_8^o YZ)$; each state $\rho_{X_8^o YZ}^{a\bar{a}\mu\mu}$ has the superselection sectors indicated on respective boundaries in the figure (after step 2).

In step 3, we smoothly deform the region “figure-8-with-2-holes” back to itself. The deformation is such that the hole with anyon sector a is transported along the figure-8 by almost a complete loop (initially moving upward), and the hole that carries \bar{a} is also transported upwards slightly. Thus regions Y and Z are stretched during step 3 and become thin (and long) immersed strips Y' and Z' . After step 3, \bar{a} is in the upper hole and a is in the lower hole of “figure-8-with-2-holes”.

Although it might sound an obvious comment, we emphasize that transporting an anyon along the immersed figure-8 (embedded in a ball or a sphere) cannot change anyon type.¹⁰ It is because

¹⁰This is a special instance of Lemma 4.3 of [14], which says no matter how we transport an annulus within a fixed large disk (keep the annulus embedded during the process) and come back to its original position, anyons cannot be permuted.

of this important property that we can conclude the argument. Suppose X_8° , Y and Z are deformed into $X_8^{\circ'}$, Y' and Z' respectively after step 3. Then the state after step 3 is

$$\tilde{\rho}'^{\mu}_{X_8^{\circ'}Y'Z'} = \frac{1}{|\mathcal{C}|} \sum_{a \in \mathcal{C}} \rho^{\bar{a}\mu\mu}_{X_8^{\circ'}Y'Z'}, \quad I(X' : Z'|Y')_{\tilde{\rho}'^{\mu}} = 0. \quad (21)$$

In fact, $\rho^{\bar{a}\mu\mu}_{X_8^{\circ'}Y'Z'} = \rho^{\bar{a}\mu\mu}_{X_8^\circ YZ}$ because we deformed the "figure-8-with-2-holes" back to itself. (The uniqueness of the state with labeling $\bar{a}\mu\mu$ follows from the fact that $a, \bar{a} \in \mathcal{C}$ are Abelian.) Thus $\tilde{\rho}'^{\mu} = \tilde{\rho}^{\mu}$. The vanishing of conditional mutual information in (21) follows from that in (20) and the fact that smooth deformation of the regions preserves the conditional mutual information.

In Step 4, we trace out the horizontal strip, and this effectively brings a and \bar{a} together. According to the Abelian fusion rule $a \times \bar{a} = 1$ (derived in entanglement bootstrap in a self-contained way), the fusion outcome must be in the vacuum sector $1 \in \mathcal{C}$. The resulting state on $X_8^\circ = ABCDE$ is nothing but the reduced density matrix of $\rho^{\mu}_{X_8}$! (Step 5 is intended to be a dummy step indicating that it is possible to fill in the hole and get a state $\rho^{\mu}_{X_8}$. This is precisely the content of the previous sentence.) Let us relabel the regions as the figure we redraw on the right, i.e., $X_8^{\circ'} \supset AE$, $Y' = BD$ and $Z' = C$. By the strong subadditivity

$$I(AE : C|BD)_{\rho^{\mu}} \leq I(X_8^{\circ'} : Z'|Y')_{\tilde{\rho}'^{\mu}} = 0. \quad (22)$$

We used the fact that $\tilde{\rho}'^{\mu}$, when reduced to X_8° , gives $\rho^{\mu}_{X_8^\circ}$. Thus, $I(AE : C|BD)_{\rho^{\mu}} = 0$.

Below, we show $I(AE : C|BD)_{\rho^{\mu}} = 0$ implies a very useful condition

$$\boxed{I(A : E|BCD)_{\rho^{\mu}} = 0.} \quad (23)$$

The steps are as follows.

$$\begin{aligned} 0 &= I(AE : C|BD)_{\rho^{\mu}} \\ &= S_{ABDE} + S_{BCD} - S_{BD} - S_{ABCDE} \\ &= (S_{AB} + S_{DE}) + (S_{BC} + S_{CD} - S_C) - (S_B + S_D) - S_{ABCDE} \\ &= (S_{AB} + S_{BC} - S_B) + (S_{DE} + S_{CD} - S_D) - S_C - S_{ABCDE} \\ &= S_{ABC} + S_{CDE} - S_C - S_{ABCDE} \\ &= I(AB : DE|C)_{\rho^{\mu}} \\ &\geq I(A : E|BCD)_{\rho^{\mu}}. \end{aligned} \quad (24)$$

In the third line, we use the fact that the extreme point $\rho^{\mu}_{X_8}$ factorizes on some region pairs such as (AB, DE) and (B, D) and the quantum Markov state condition $I(B : D|C)_{\rho^{\mu}} = 0$. In the fifth line, we used $I(A : C|B)_{\rho^{\mu}} = 0$ and $I(C : E|D)_{\rho^{\mu}} = 0$. The last line follows from strong subadditivity. Thus, Eq. (23) holds. Then, by Lemma 4 (item 4 \Rightarrow item 0), any $\mu \in \mathcal{C}_8$ is Abelian. \square

The key ingredient of the above proof is that transporting an anyon along the figure-8 does not change its type; here, we assume that the figure-8 region is immersed in a ball or a sphere. We emphasize again that the crucial input is the anyon transportation property in the neighborhood of the immersed region, and it is not essential to assume the immersion is in a ball or sphere if we know this property. This observation will be useful later in Section 5.

The special property of Abelian anyon theory we make use of is the deterministic fusion outcome $a \times \bar{a} = 1$. Because of this, the proof idea cannot be generalized easily to non-Abelian theories. One may wonder if a careful analysis of the fusion spaces involving multiple sectors in \mathcal{C} and \mathcal{C}_8 can be helpful in the general case. A complementary idea is to try to take full advantage of the fact that the figure-8 annulus is immersed in a sphere. We leave the general case as an open problem.

5 Transportation experiment

We discuss a thought experiment, “transportation experiment,” which reveals the physical connection between immersed annuli with topological defects. The entanglement bootstrap setup in this section is relaxed compared with that in Sections 3 and 4. Let us consider 2D for simplicity. We allow the reference state to have “defect points” where the axioms may be violated. (Alternatively, we consider a reference state defined on a manifold N with nontrivial topology, e.g., a k -hole disk.) The setup is illustrated in Fig. 9.

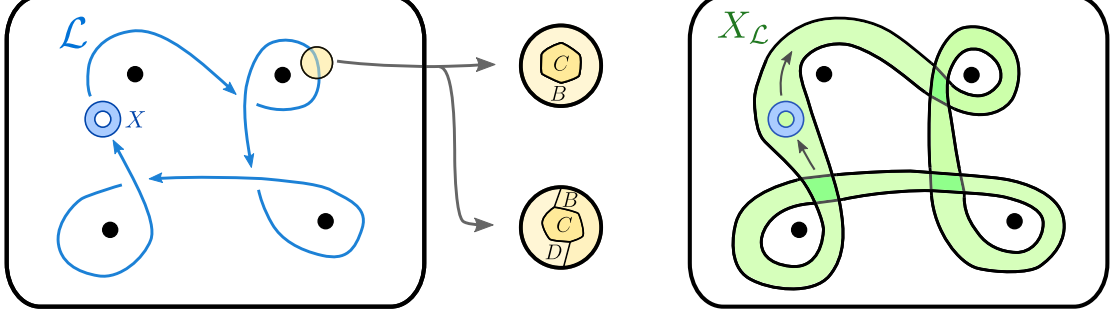


Figure 9: The entanglement bootstrap setup of Section 5 and the main idea of the “transportation experiment”. The black dots in the figure are places we do not impose the axioms. The loop \mathcal{L} along which we transport the “test annulus” (blue) is away from these black dots. The thickening of \mathcal{L} denoted by $X_{\mathcal{L}}$ (green) is an immersed annulus.

We want to transport an anyon along a closed loop \mathcal{L} and back. In entanglement bootstrap, this is done by transporting a “test annulus” X , which is a sufficiently small embedded annulus that detects the anyon type by the information convex set $\Sigma(X)$. If we transport the test annulus X along closed loop \mathcal{L} and back to its original position, we have an automorphism of the information convex set determined by the loop \mathcal{L} .¹¹

$$\Phi(\mathcal{L}) : \Sigma(X) \rightarrow \Sigma(X). \quad (25)$$

In general, the automorphism $\Phi(\mathcal{L})$ can permute extreme points of $\Sigma(X)$, and thus, it permutes anyon types. In other words, for each \mathcal{L} , we have an automorphism of labels $\varphi_{\mathcal{L}} : \mathcal{C} \rightarrow \mathcal{C}$. The automorphism depends only on the topological class of \mathcal{L} , i.e., smoothly deforming \mathcal{L} without passing the defect points preserves Φ and φ . Explicit examples come from topological defects, which we recall in Section 5.1. Throughout this section, we consider loops \mathcal{L} whose thickening ($X_{\mathcal{L}}$) is an immersed annulus.¹² We define

$$\mathcal{I}(\mathcal{L}) \equiv \{a \in \mathcal{C} \mid a = \varphi_{\mathcal{L}}(a)\} \quad (26)$$

as the subset of superselection sectors in \mathcal{C} that are preserved under the automorphism. Therefore, $|\mathcal{I}(\mathcal{L})| = |\mathcal{C}|$ if and only if no anyons are permuted. We let $\mathcal{C}_{\mathcal{L}}$ be the set of superselection sectors associated with the extreme points of $\Sigma(X_{\mathcal{L}})$.

Definition 8 (parallel transportation). Transportation along \mathcal{L} is parallel if $|\mathcal{I}(\mathcal{L})| = |\mathcal{C}|$.

In this section, we ask the following questions.

$$\text{Question:} \quad |\mathcal{I}(\mathcal{L})| = |\mathcal{C}| \quad \stackrel{?}{\iff} \quad \exists \mu \in \mathcal{C}_{\mathcal{L}} \text{ s.t. } d_{\mu} = 1. \quad (27)$$

¹¹Accurately speaking, the automorphism is determined by a loop \mathcal{L} with a chosen orientation. We may denote an oriented loop as $\vec{\mathcal{L}}$. However, we shall use \mathcal{L} for simplicity. Quantities of interest below, such as the subset of anyons not permuted by the transportation, do not depend on the orientation. (For a discussion of automorphisms of information convex sets in broader setups, see Appendix B.)

¹²This excludes some loops on nonorientable manifolds. For instance, the noncontractible loop on RP^2 can be thickened to an Möbius strip but not an annulus.

We explain why the “ \Leftarrow ” direction is a relatively simple fact (Proposition 10). We conjecture that the statement is true in the “ \Rightarrow ” direction (Conjecture 11). We explain the fact that “ \Rightarrow ” is true for Abelian anyon theories, adopting the discussion in Section 4 to this context. Note that Conjecture 11 implies the existence of an Abelian sector on the figure-8 annulus as a special case; thus, it also implies the strong isomorphism conjecture in 2D. Another result is Proposition 9, which states $|\mathcal{C}_{\mathcal{L}}| = |\mathcal{I}(\mathcal{L})|$. It implies $|\mathcal{C}_8| = |\mathcal{C}|$ as a special case.

5.1 Topological defects: an example

A well-known example of topological defect is the one that permutes e and m in the toric code model [34]. The anyon types of the toric code are $\mathcal{C} = \{1, e, m, f\}$. Their quantum dimensions are $d_1 = d_e = d_m = d_f = 1$. Topological defects in this model are non-Abelian $\mathcal{C}' = \{\sigma_+, \sigma_-\}$ with $d_{\sigma_+} = d_{\sigma_-} = \sqrt{2}$. Anyons e and m are permuted when they are transported around the defect (either σ_+ or σ_-). While defects are most familiar in the context where global symmetries are present [35], it is understood that the phenomenon of permuting anyons does not go away under arbitrary local perturbations, not preserving any symmetry.

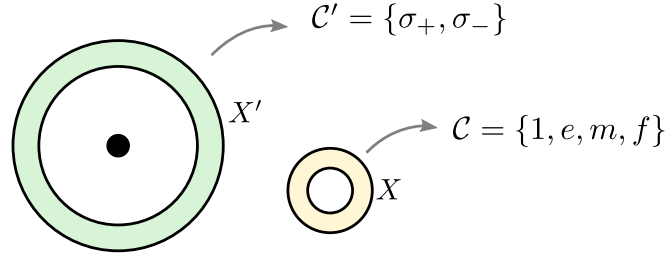


Figure 10: Information convex set is affected by the presence of a defect (black dot). The illustration is for the toric code with a defect that permutes e and m .

The presence of a defect affects information convex sets. This is illustrated in Fig. 10 for the toric code example. The annulus X' surrounds the defect, and its information convex set $\Sigma(X')$ has two extreme points. The quantum dimension for each extreme point, defined according to Definition 1, agrees with $d_{\sigma_+} = d_{\sigma_-} = \sqrt{2}$. Thus, no Abelian sector exists on annulus X' . If we consider an embedded annulus X not surrounding any defect, then the information convex set $\Sigma(X)$ is a simplex with four extreme points. These extreme points correspond to Abelian sectors 1, e , m , and f . The model is solvable, and explicit computation¹³ can be done to verify these statements. Putting aside the details, examples like this are nontrivial contexts for question (27).

5.2 Constraints of transportation

Below, we analyze the constraints of the transportation problem (Fig. 9). The entanglement bootstrap setup and notations have been described at the beginning of the section. As a useful fact, we note $1 \in \mathcal{I}(\mathcal{L})$. This is because the test annulus X remains embedded in the entire process, and we can reversibly fill in the hole at any step if it carries the vacuum sector $1 \in \mathcal{C}$. We start with a general statement:

Proposition 9. $|\mathcal{C}_{\mathcal{L}}| = |\mathcal{I}(\mathcal{L})|$. In particular, if the transportation is parallel, $|\mathcal{C}_{\mathcal{L}}| = |\mathcal{C}|$.

As a corollary, $|\mathcal{C}| = |\mathcal{C}_8|$. This is because transporting an anyon along a figure-8 immersed in a ball or sphere cannot change the anyon type.

¹³Similar computation can be done in some non-Abelian models, such as quantum double using “minimum diagram” technique [16, 36].

Here is a sketch of the key idea of proof of Prop. 9. The trick is to attach the test annulus to another annulus by a strip. After transporting the test annulus, the strip will be stretched along loop \mathcal{L} . After gluing the test annulus with the other annulus (by merging with another annulus), we get a punctured torus $\mathcal{W}_{\mathcal{L}}$. This process is illustrated in Fig. 11. The main part of the proof is to analyze $\Sigma(\mathcal{W}_{\mathcal{L}})$, or more conveniently $\Sigma(T^2)$, where the torus T^2 has a reference state obtained by an analog of “vacuum block completion” (see Example 4.27 of [17]).

Proof. Consider the process illustrated in Fig. 11. We start with a disk away from the defect points (black dots) and remove two small balls from it. Let the resulting 2-hole disk be Y . Consider a state labeled by $a, 1, a$ on the three boundaries $\rho_Y^{a1a} \in \Sigma(Y)$. It must be an extreme point because the corresponding fusion space is 1 dimensional.

In step 1, we move the annulus that carries $a \in \mathcal{C}$ (the test annulus we choose) upwards so that the region Y is deformed into an immersed region Y' . One of the boundaries of Y' is now labeled by $\hat{1}$, indicating that it is the vacuum sector deformed onto an immersed annulus, so we cannot compare the state directly to the reference state. A fact useful later is that $\hat{1}$ is Abelian. In step 2, we transport the test annulus further along the closed loop \mathcal{L} and call the resulting region $Y_{\mathcal{L}}$, as illustrated in Fig. 11(c).

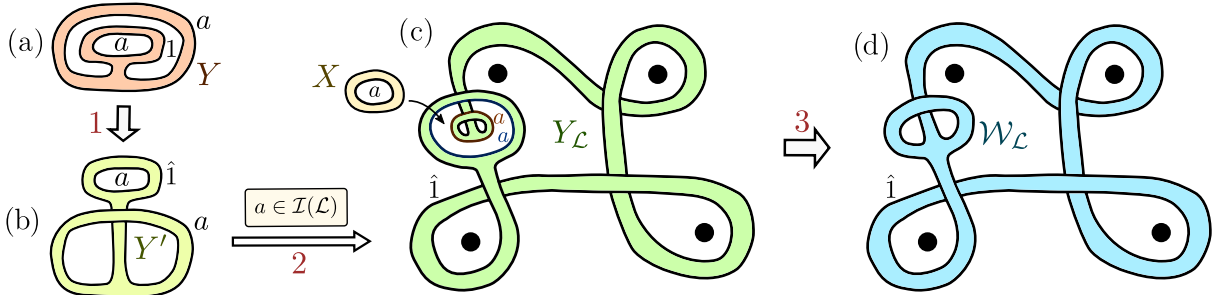


Figure 11: Construction of an extreme point in $\Sigma_{\hat{1}}(\mathcal{W}_{\mathcal{L}})$, useful in the proof of Prop. 9.

If $a \in \mathcal{I}(\mathcal{L})$, that is, a is invariant under the transportation along \mathcal{L} , we do step 3 of Fig. 11, which glues annulus X with the state on $Y_{\mathcal{L}}$ to a punctured torus $\mathcal{W}_{\mathcal{L}}$. In terms of quantum states, we merge two quantum states, which are extreme points of $\Sigma(X)$ and $\Sigma(Y_{\mathcal{L}})$ (thickening a certain region before merging if needed) with the superselection sectors labeled in Fig. 11(c). Here, $a \in \mathcal{I}(\mathcal{L})$ is required so that the two states match on their overlap regions. For each valid choice of a , we get an extreme point of $\Sigma_{\hat{1}}(\mathcal{W}_{\mathcal{L}})$. Note that $1 \in \mathcal{I}(\mathcal{L})$, and therefore $\Sigma_{\hat{1}}(\mathcal{W}_{\mathcal{L}})$ is nonempty. Note that the punctured torus $\mathcal{W}_{\mathcal{L}}$ contains annuli $X_{\mathcal{L}}$ and an embedded test annulus X .

Next, we “complete” $\mathcal{W}_{\mathcal{L}}$ into a torus T^2 with a valid reference state. This step is optional, but it is both natural and convenient. The details are as follows. Choose $a = 1$, and run the process in Fig. 11 to obtain an extreme point $\rho_{\mathcal{W}_{\mathcal{L}}}^{1_X} \in \Sigma_{\hat{1}}(\mathcal{W}_{\mathcal{L}})$. By the completion trick (Lemma 4.4 of [17]), we first thicken $\mathcal{W}_{\mathcal{L}}$ and then heal the puncture. By doing this, we obtain a pure state $|1_X\rangle$ on a torus T^2 . By construction, $T^2 \supset \mathcal{W}_{\mathcal{L}}$, and because $\hat{1}$ on the thickened boundary of $\mathcal{W}_{\mathcal{L}}$ is Abelian, $|1_X\rangle$ is a valid reference state: it satisfies **A0** and **A1** everywhere. (The notation $|1_X\rangle$ is a reminder that if we reduce it to X , we get the reference state σ_X .)

Having explained the construction, we explain various constraints on the information convex sets, which leads to the conclusion. First, by applying the associativity to step 3 (combining X and $Y_{\mathcal{L}}$ into $\mathcal{W}_{\mathcal{L}}$), we have $\dim \mathbb{V}_{\hat{1}}(\mathcal{W}_{\mathcal{L}}) = |\mathcal{I}(\mathcal{L})|$, this is by counting the number of ways to match the boundary conditions in Fig. 11. If we take the reference state $|1_X\rangle$ on the “completed” torus T^2 , we further have $\dim \mathbb{V}(T^2) = |\mathcal{I}(\mathcal{L})|$. This equality is easy to understand from the point of view that $T^2 = X\bar{X}$, where \bar{X} is the complement of X on T^2 . Both X and \bar{X} are annuli and sectorizable.

Applying the associativity to the gluing of the two annuli, we have

$$\dim \mathbb{V}(T^2) = \sum_{a,b \in \mathcal{C}} \delta_{a,b} \delta_{a,\varphi_{\mathcal{L}}(b)} = |\mathcal{I}(\mathcal{L})|, \quad (28)$$

where $\delta_{a,b}$ comes from the matching of sector on one shared boundary of the two annuli, and $\delta_{a,\varphi_{\mathcal{L}}(b)}$ comes from the other shared boundary. The appearance of $\varphi_{\mathcal{L}}$ is due to the transportation property.

Similarly, we cut the torus along another direction into two annuli, $T^2 = X_{\mathcal{L}} \bar{X}_{\mathcal{L}}$. Here, $X_{\mathcal{L}}$ is the immersed annulus that thickens \mathcal{L} , a notation explained in Fig. 9. Not only are $X_{\mathcal{L}}$ and $\bar{X}_{\mathcal{L}}$ both sectorizable, but they must also have isomorphism information convex sets $\Sigma(X_{\mathcal{L}}) \cong \Sigma(\bar{X}_{\mathcal{L}})$. This is because $X_{\mathcal{L}}$ deforms to $\bar{X}_{\mathcal{L}}$ smoothly on T^2 . So they both characterize $\mathcal{C}_{\mathcal{L}}$. From a computation parallel to Eq. (28), we see

$$\dim \mathbb{V}(T^2) \leq |\mathcal{C}_{\mathcal{L}}|. \quad (29)$$

The possibility to have “<” is associated with the possibility that only a subset of labels in $\mathcal{C}_{\mathcal{L}}$ survive the matching and appear on the torus. In particular, if “<” applies, we cannot obtain the maximum-entropy state in $\Sigma(X_{\mathcal{L}})$ by a partial trace from any state in $\Sigma(T^2)$.

Below, we show “=” in Eq. (29) must be realized. This is done by explicitly finding a state in $\Sigma(T^2)$ that reduces to the maximum-entropy state of $\Sigma(X_{\mathcal{L}})$. The state we identify is precisely $|1_X\rangle$. (The logic below is familiar. See, e.g., Lemma 5.7 of [17].) Recall that $|1_X\rangle$ reduces to the test annulus X gives the vacuum state $\rho_X^1 \equiv \sigma_X$, an Abelian extreme point. Now apply the definition of quantum dimension (8) to the partition of $X = BCD$ as Fig. 3, with the requirement that $B = \partial X \cap X_{\mathcal{L}}$. By strong subadditivity,

$$0 = \Delta(B, C, D)_{|1_X\rangle} \geq I(\bar{X} : C|B)_{|1_X\rangle} \geq I(A : C_-|B)_{|1_X\rangle}, \quad (30)$$

for any $A \subset \bar{X}$ and $C_- \subset C$. The specific choice $A = X_{\mathcal{L}} \setminus X$ and $C_- = X_{\mathcal{L}} \cap (X \setminus \partial X)$ is what we want because ABC_- is now a Levin-Wen partition [23] of the immersed annulus $X_{\mathcal{L}}$ (namely, A and C_- are two disks, and they are separated by B). $I(A : C_-|B)_{|1_X\rangle} = 0$ for the Levin-Wen partition [2] of $X_{\mathcal{L}}$ implies that $|1_X\rangle$ reduces to $X_{\mathcal{L}}$ is the maximum-entropy state of $\Sigma(X_{\mathcal{L}})$. This implies “=” applies to Eq. (29). \square

Proposition 10. *If there exists $\mu \in \mathcal{C}_{\mathcal{L}}$ with $d_{\mu} = 1$, the transportation along \mathcal{L} is parallel.*

Proof. An annulus is a disk with a puncture, homeomorphically speaking. If the state on $X_{\mathcal{L}}$ is an extreme point, we can use the completion trick (Lemma 4.4 of [17]) to heal a puncture to obtain a state on the disk. The resulting state satisfies the axioms on the entire disk if the extreme point is associated with an Abelian sector ($\mu \in \mathcal{C}_{\mathcal{L}}$ with $d_{\mu} = 1$). Let this state be $\tilde{\sigma}$. It is known that transporting a test annulus on a disk cannot permute anyon types, supposing that the disk has a reference state. (This is by Lemma 4.3 of [14]). As the loop $X_{\mathcal{L}}$ is identified as part of the disk for which we have a valid reference state $\tilde{\sigma}$, the transportation of test annulus on $X_{\mathcal{L}}$ cannot permute anyons. Thus, the transportation along \mathcal{L} is parallel. \square

Conjecture 11. *If the transportation along \mathcal{L} is parallel, there exists $\mu \in \mathcal{C}_{\mathcal{L}}$ with $d_{\mu} = 1$.*

Proof of conjecture 11 for Abelian anyon theories. For Abelian anyon theory (that is $d_a = 1$ for $\forall a \in \mathcal{C}$), the conjecture holds. The proof is that of Proposition 7, with a few minor and easy-to-state modifications. We only need to replace the immersed figure-8 annulus in Fig. 8 with the immersed annulus $X_{\mathcal{L}}$ in Fig. 9. As we noted, every step works here because nowhere in the proof of Proposition 7 did we use the condition that the annulus is immersed in a sphere. All we needed was the fact that a test annulus carrying $\forall a \in \mathcal{C}$ transported along the immersed annulus remains in the same superselection sector a . For Abelian anyon theory, what we prove is $d_{\mu} = 1$ for *any* $\mu \in \mathcal{C}_{\mathcal{L}}$. \square

We do not have proof of the general case. This conjecture implies Conjecture 5, and thus, it also implies the 2-dimensional strong isomorphism conjecture (Conjecture 6).

6 Discussion

In this work, we started by asking a simple question: “is there an Abelian superselection sector detected by the immersed figure-8 annulus?” The question is relevant to gapped topologically ordered systems in 2D, which support anyons and is formulated in the framework of entanglement bootstrap. We gave an affirmative answer to this question for Abelian anyon theories but leave the general case as a conjecture (Conjecture 5). We explained the fact that if there is an Abelian sector on figure-8, a certain strong isomorphism (Conjecture 6) of information convex sets must be true: if two homeomorphic regions Ω and Ω' are immersed in the sphere or a disk, the information convex sets $\Sigma(\Omega)$ and $\Sigma(\Omega')$ must be isomorphic. Importantly, it does not matter if Ω can be smoothly deformed to Ω' on the sphere (or disk), a situation where the established isomorphism theorem does not apply.

If the conjecture of the existence of an Abelian sector on “figure-8” annulus turns out false, a counterexample (e.g., a solvable model) would be extremely interesting. This also means the existence (absence) of Abelian sectors on immersed figure-8 will be a nontrivial (and exotic) criterion for classifying wave functions with entanglement area law as well as topologically ordered phases.

Suppose the existence of an Abelian sector on figure-8 (Conjecture 5) can be proved. Strong isomorphism will be a fact. While strong isomorphism is powerful, it seems to imply that we cannot learn much by looking at a topological space immersed differently. Let me argue this is far from the case. If strong isomorphism holds, a couple of intriguing questions can be pursued. In particular, it means tunneling processes (Section 3.1 and Fig. 5) can generate explicit isomorphisms not allowed by smooth deformation. Thus, automorphisms of information convex sets will not only come from topologically nontrivial ways to smoothly deform an immersed region back to itself but also from ways that utilize tunneling in intermediate steps. We expect these diverse topological classes of automorphisms to be informative. A natural question is: “Can we use these automorphisms (dancing of quantum states) to extract all the data of the modular tensor category underlying an anyon model?”¹⁴ If the answer is affirmative, it will manifestly use a single quantum state, and this will be complementary to the “microscopic approach” [37]. Can the mathematical structure coming out of immersion be comparable with the mapping class group? Analogous questions in higher dimensions can be asked in parallel and are more open.

A stronger conjecture we postponed until now is the existence of a canonical (Abelian) vacuum state on the immersed figure-8 annulus. If this is true, the process in Fig. 15 of the appendix may well be on the right track in extracting the full set of anyon topological spins. This is a meaningful problem that deserves an effort elsewhere. Proving the existence of a canonical vacuum on figure-8 remains an open problem, even for Abelian anyon theories, in which context we proved Conjecture 5.

We further discussed the relevance of immersed annuli in contexts with topological defects. The central question we asked was Eq. (27), relating “parallel” transportation to the existence of an Abelian sector on the immersed annulus that thickens the transportation loop. The question has two directions, and we provided an affirmative answer to one direction. The other direction is a conjecture that implies our main conjecture about the existence of an Abelian state on figure-8 (Conjecture 5) as well as strong isomorphism.

Although this work focuses on 2D, we expect that the insights gained are useful in higher dimensions as well. Questions stirring in the right direction could be: what are generalizations of the tunneling trick (Section 3.1 and Fig. 5) and transportation experiments (Section 5 and Fig. 9) in higher dimensions? We developed some tools and discussed a few further open problems for higher dimensions in the appendices.

Finally, we ask whether considering quantum states on regions immersed in a physical system can be useful in other physical contexts. Immersed regions utilize the Hilbert space more efficiently by

¹⁴An optimism to this possibility was found independent by Kyle Kawagoe, who attended my chalk talk at math department Ohio State University.

using local pieces more than once, and they can be made larger and topologically (or geometrically) more interesting than the original physical system available to us. Smooth deformation of immersion region, a property natural in systems with entanglement area law, will be absent in broader contexts such as gapless systems. Nevertheless, many other benefits of immersion may persist.

Acknowledgments

After settling the Abelian case, I made multiple attempts on the general proof of Conjecture 5 without progress. These years gave me the time to contemplate the potential implications of this conjecture, especially strong isomorphism and tunneling. Conversations with many helped me sharpen these thoughts, including Anuj Apte, Yu-An Chen, Tarun Grover, Isaac Kim, Xiang Li, Ting-Chun Lin, Hanqing Liu, Daniel Ranard, Hao-Yu Sun, Chong Wang, Xueda Wen, and Carolyn Zhang. I thank John McGreevy and Jin-Long Huang for collaborating on projects that taught me immersion-related topology. I thank Michael Levin for a conversation about topological spin during a UQM conference at Caltech in 2022 and an intriguing discussion with John McGreevy on a train to that conference. I thank my classmate Yang Fan for sharing the video “outside in” [29] with me many years ago. I thank Xinyao Zhao for providing a selection of colors, some of which I chose for some figures. I thank Ilya Gruzberg, Kyle Kawagoe, Yuan-Ming Lu, David Penneys, and Stuart Raby for related conversations during my visit to Ohio State University near the completion of this work. This work was supported by the Simons Collaboration on Ultra-Quantum Matter, a grant from the Simons Foundation (652264).

A Equivalent definitions of quantum dimension

Immersed sphere shells, in the context of n -dimensional entanglement bootstrap, are sectorizable regions. We derive an equivalence relation on the definition of quantum dimensions (Lemma 12) for immersed sphere shells in n -dimensions, where $n \geq 2$ and is arbitrary. It applies to immersed annuli as a special case ($n = 2$).

Because the setup is general, we introduce some diagrammatic notation for the partitions. Let $Z = S^{n-1} \times \mathbb{I}$ be a sphere shell in n space dimensions, where S^{n-1} is a $(n-1)$ -sphere and \mathbb{I} is an interval. In Fig. 12, the horizontal direction indicates the direction of the interval \mathbb{I} . Therefore, each vertical strip that connects the top and the bottom represents a sphere shell. If a strip is cut in half (top and bottom), each piece is a half-sphere shell (topologically a ball). We denote the superselection sectors detected by $\Sigma(Z)$ as \mathcal{C}_Z .

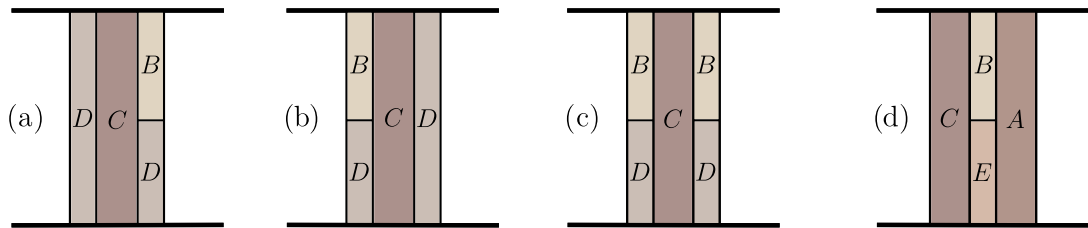


Figure 12: Partitions of a sphere shell $Z = S^{n-1} \times \mathbb{I}$. The horizontal direction is the direction of the interval \mathbb{I} .

Lemma 12. *The following are equivalent definitions of quantum dimension d_h of $h \in \mathcal{C}_Z$, where Z is an immersed sphere shell in n -dimension.*

(a) $\Delta(B, C, D) = 2 \ln d_h$ for the partition in Fig. 12(a).

(b) $\Delta(B, C, D) = 2 \ln d_h$ for the partition in Fig. 12(b).

(c) $\Delta(B, C, D) = 4 \ln d_h$ for the partition in Fig. 12(c).

(d) $I(A : C|B) = 2 \ln d_h$ for the partition in Fig. 12(d).

Remark. We shall see in the proof that we do not need to deform the annulus. Therefore, Lemma 12 holds not only for sphere shells immersed in a sphere but also applicable to contexts allowing topological defects (i.e., when the reference state is on a manifold with a nontrivial topology).

Proof. First, we consider the partition in Fig. 13(a), where $Z = ABCDEF$. By the strong subadditivity, $\Delta(B, C, DE)_{\rho^h} \geq I(A : C|B)_{\rho^h}$. Furthermore, because ρ_Z^h is an extreme point of $\Sigma(Z)$, it factorizes as $\rho_{BCDEF}^h = \rho_{BCDE}^h \otimes \rho_F^h$, which implies

$$\Delta(B, C, DE)_{\rho^h} = \Delta(B, C, DEF)_{\rho^h}. \quad (31)$$

The region Z , as a sectorizable region, satisfies $\Delta(\partial Z, Z \setminus \partial Z)_{\rho^h} = 0$, the so-called “extreme point criterion”. It implies

$$\begin{aligned} S_{CDEF} &= S_Z + S_{AB}, \\ S_{DEF} &= S_Z + S_{ABC}, \end{aligned} \quad (32)$$

where the first line follows letting ∂Z be $CDEF$. The second line uses $0 = \Delta(EF, ABCD) \geq \Delta(DEF, ABC)$.

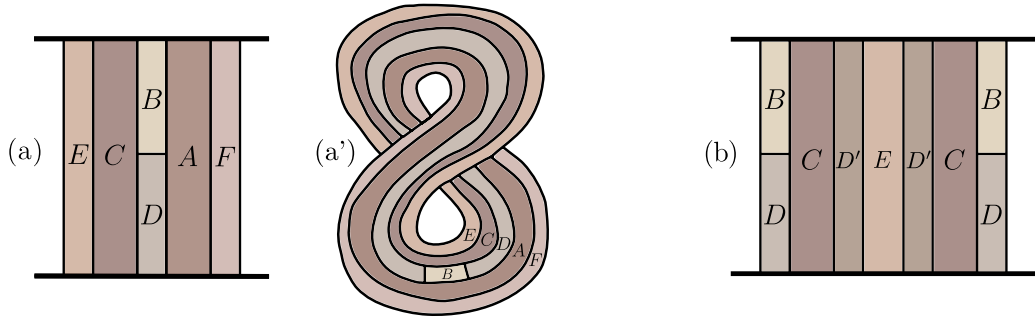


Figure 13: Partitions used in the proof of Lemma 12. In (a) and (b), the convention is the same as that in Fig. 12. (a') illustrates the partition of (a) in the concrete case that $Z = X_8$ is the “figure-8”.

Therefore, combining (31) and (32), we get

$$\begin{aligned} \Delta(B, C, DE)_{\rho^h} &= \Delta(B, C, DEF)_{\rho^h} \\ &= (S_{BC} - S_B + S_{CDEF} - S_{DEF})_{\rho^h} \\ &= (S_{BC} - S_B + S_{AB} - S_{ABC})_{\rho^h} \\ &= I(A : C|B)_{\rho^h}. \end{aligned} \quad (33)$$

Thus, among the statements in Lemma 12, (a) and (d) are equivalent. Similarly, (b) and (d) are equivalent. Therefore, the three statements (a), (b), and (d) in Lemma 12 are equivalent.

The next step is establishing the equivalence between statement (c) and the rest. For this purpose, we consider Fig. 13(b), where $Z = BCDD'E$. We will show:

$$\Delta(B, CD'E, D)_{\rho^h} = \Delta(B, C, DD')_{\rho^h}. \quad (34)$$

Then, because the extreme point ρ_Z^h factorizes as a tensor product on the left of E and right of E , we have $\Delta(B, CD'E, D)_{\rho^h} = \Delta_L + \Delta_R$. Δ_L and Δ_R give contributions identical to conditions (a) and (b) of Lemma 12. Thus, the claimed result holds.

The rest of the proof is the justification of (34). In fact, this is a special case of the decoupling lemma (Lemma D.1 of [16]). Nonetheless, we spell out the details so readers do not need to read the more general decoupling lemma.

All regions below are those in Fig. 13(b). Because ρ_Z^h is an extreme point, it satisfies

$$\begin{aligned} S_{BCD'E} &= S_{BC} - S_C + S_{CD'E} \\ S_{CDD'E} &= S_{CDD'} - S_{D'} + S_{D'E} \\ S_D + S_{D'} &= S_{DD'} \\ 0 &= S_{CD'E} - S_C + S_{D'E}. \end{aligned} \tag{35}$$

The first and second lines follow from the vanishing of conditional mutual information, bounded by the extreme point criterion: (1st line) $0 = \Delta(C, D'E)_{\rho^h} \geq I(B : D'E|C)_{\rho^h}$, (2nd line) $0 = \Delta(D', E)_{\rho^h} \geq I(CD : E|D')_{\rho^h}$. The third line is because any extreme point is factorized into a tensor product along disjoint shells arranged in the interval \mathbb{I} direction. The fourth line is $\Delta(C, D'E)_{\rho^h} = 0$, also by the extreme point criterion. Therefore,

$$\begin{aligned} \Delta(B, CD'E, D)_{\rho^h} &= S_{BCD'E} + S_{CDD'E} - S_B - S_D \\ &= (S_{BC} - S_C + S_{CD'E}) + (S_{D'E} - S_{D'} + S_{CDD'}) - S_B - S_D \\ &= S_{BC} + (S_{CD'E} - S_C + S_{D'E}) + S_{CDD'} - S_B - (S_{D'} + S_D) \\ &= S_{BC} + S_{CDD'} - S_B - S_{DD'} \\ &= \Delta(B, C, DD')_{\rho^h}. \end{aligned} \tag{36}$$

The brackets in the middle steps are replacements according to Eq. (35). This completes the proof. \square

Lemma 12 implies that $d_h \geq 1$, for any superselection sector h detected by a sphere shell. Such superselection sectors are associated with point excitations. It is worth noting that, in $n \geq 3$, not every type of superselection sector is associated with point excitations, and many of them are not detected by sphere shells. The general definition of quantum dimension for immersed sectorizable regions is currently lacking. Nonetheless, a generalization is known for regions participating in a pairing [17].

B Automorphism of information convex sets: tools and examples

Automorphism (i.e., self-isomorphism) of information convex sets plays an important role in entanglement bootstrap. The simplest application is the definition of antiparticles, but its implication is much broader. In this appendix, we talk about two things related to automorphisms of information convex sets.

In Section B.1, we introduce a “immersion complex” $\mathfrak{M}(\omega, N)$ (Definition 13). It is a simplicial complex whose points represent immersed regions. It is an attempt to provide a compact mathematical way to describe two things: (i) topological classes of immersion (ω into N) by counting the connected component (π_0) of \mathfrak{M} , and (ii) the topological classes of deformation of an immersed region $\Omega \looparrowright N$ back itself (keeping the intermediate configurations immersed), as the fundamental group (π_1) of a connected component of \mathfrak{M} . In Section B.2, we utilize tunneling (Section 3.1) to make automorphisms not available otherwise.

B.1 Math related to immersion and deformation classes

Consider the immersion of an n -dimensional space with boundary into another, $\Omega \looparrowright N$. Let the homeomorphism class of Ω be ω . In our convention, Ω knows all the data of the immersed

region while ω forgets everything but the homeomorphism class. (We intend to first describe the mathematical problem and postpone the physical relevance to automorphisms of information convex sets and examples in the latter part of the section.)

Let $\mathcal{R}(\omega, N) = \{\Omega_1(\omega), \Omega_2(\omega), \dots\}$ be the set of representatives of equivalence classes of immersion of ω into N . That is

1. $\Omega_i(\omega) \looparrowright N$ for any i ;
2. $\Omega_i(\omega) \not\stackrel{N}{\sim} \Omega_j(\omega)$ if $i \neq j$;
3. $\Omega_i(\omega)$ is homeomorphic to ω for any i ;
4. any $\Omega \looparrowright N$ homeomorphic to ω must satisfy $\Omega \stackrel{N}{\sim} \Omega_i(\omega)$ for some i .

Here, $Y \stackrel{N}{\sim} Z$ means two immersed regions $Y, Z \looparrowright N$ can be smoothly deformed to each other on N , where the intermediate configurations are immersed. In particular, if there is no way to immerse ω to N , $\mathcal{R}(\omega, N) = \emptyset$. Now we are ready to introduce the “immersion complex”.

Definition 13 (Immersion complex). Let ω and N be two n -dimensional manifolds, possibly with boundaries. We define the immersion complex $\mathfrak{M}(\omega, N)$ as

$$\mathfrak{M}(\omega, N) \equiv \coprod_{\Omega \in \mathcal{R}(\omega, N)} \mathfrak{m}(\Omega, N). \quad (37)$$

Here, \coprod means disjoint union, and $\mathfrak{m}(\Omega, N)$, for any $\Omega \looparrowright N$, is the simplicial 2-complex such that

1. $\Omega' \looparrowright N$ represents a point (0-simplex) of $\mathfrak{m}(\Omega, N)$ if and only if $\Omega' \stackrel{N}{\sim} \Omega$.
2. Two distinct points $\Omega, \Omega' \in \mathfrak{m}(\Omega, N)$ are connected by a 1-simplex¹⁵ of $\mathfrak{m}(\Omega, N)$ if and only if $\Omega \cap \Omega'$ can be converted to Ω and Ω' by two sequences of extensions (one for each).
3. Three distinct points $\Omega', \Omega'', \Omega''' \in \mathfrak{m}(\Omega, N)$ are connected by a triangle (2-simplex) of $\mathfrak{m}(\Omega, N)$ if and only if both of the following holds
 - $\Omega \cap \Omega' \cap \Omega''$ can be converted to $\Omega \cap \Omega'$, $\Omega' \cap \Omega''$ and $\Omega \cap \Omega''$ by three sequences of extensions (one for each).
 - Points in each of the three pairs (Ω, Ω') , (Ω', Ω'') and (Ω, Ω'') are connected by a 1-simplex of $\mathfrak{m}(\Omega, N)$, according to rule 2 above.

Remark. We emphasize that the definition above serves as an attempt to formulate the mathematical problem, but we do not claim it has the desired mathematical rigor. Even if it does, we do not know if it is the most convenient to work with. In practice, it is likely to be useful to take some cellular decomposition of manifold N and only consider only “large but finite-sized” immersed regions Ω . By doing so, the number of 1-simplex connecting a given point will be finite. (This setup is also similar to entanglement bootstrap, where the manifold N will be interpreted as the manifold on which we define the reference state, and thus N is equipped with a coarse-grained lattice.)

By definition $\mathfrak{m}(\Omega, N) = \mathfrak{m}(\Omega', N)$ if $\Omega' \stackrel{N}{\sim} \Omega$. Furthermore, $\mathfrak{m}(\Omega, N)$ must be connected. Therefore, $\mathfrak{M}(\omega, N)$ is the disjoint union of these connected components. Also, by definition, for any triangle of $\mathfrak{m}(\Omega, N)$, its three edges must be included in $\mathfrak{m}(\Omega, N)$, and for any 1-simplex of $\mathfrak{m}(\Omega, N)$ its two endpoints must be included in $\mathfrak{m}(\Omega, N)$. This means both $\mathfrak{m}(\Omega, N)$ and $\mathfrak{M}(\omega, N)$ are simplicial 2-complexes.

¹⁵A 1-simplex is a line segment connecting two points. One may alternatively call it a 1-cell.

Remark. One may ask if it is meaningful to add higher dimensional k -simplexes ($k \geq 3$) instead of stopping at $k = 2$. The relevance to physics we can think of so far (as we explain shortly) depends on π_0 and π_1 . Adding higher dimensional simplexes will not change them. Nonetheless, it remains an interesting question if higher homotopy (or homology) groups of \mathfrak{M} can provide further information.¹⁶

B.1.1 Physical relevance of immersion complex through the homotopy groups

It is easy to explain why the number of connected components π_0 of $\mathfrak{M}(\omega, N)$ is of physical relevance. Consider the entanglement bootstrap setup where N is the manifold on which we define our reference state σ_N . The n -dimensional version of axioms **A0** and **A1** are satisfied everywhere on N . Then $\pi_0(\mathfrak{M}(\omega, N))$, i.e., the number of connected components of $\mathfrak{M}(\omega, N)$, is the number of inequivalent immersions of the topological space ω in N . For instance, $\pi_0(\mathfrak{M}(\text{annulus}, S^2))$ is \mathbb{Z}_2 (the cyclic group of order 2). We discussed this in the main text without using this notation. In broader contexts, $\pi_0(\mathfrak{M})$ is the set of regular homotopy class of immersed regions, which has been a topic of study in math literature; see, e.g., [38, 39, 28]. Within each connected component, $\mathfrak{m}(\Omega, N)$, $\Omega \in \mathcal{R}(\omega, N)$, we can smoothly deform the region and the isomorphism theorem implies that such deformation preserves the information convex set. Configurations in two connected components are harder to relate, although tunneling (Section 3.1) provides one way to generate isomorphisms between such configurations (when a certain Abelian sector exists).

The fundamental group of the connected components of \mathfrak{M} , i.e., $\pi_1(\mathfrak{m}(\Omega, N))$, by (37) is relevant to the study of automorphism of information convex sets:

- Immersed regions up to small deformations are represented by nearby points connected by 1-simplex in $\mathfrak{m}(\Omega, N)$. For each oriented loop $\vec{\gamma}$ in $\mathfrak{m}(\Omega, N)$ that starts at Ω and ends at Ω , we have an associated automorphism:

$$\Phi(\vec{\gamma}) : \Sigma(\Omega) \rightarrow \Sigma(\Omega). \quad (38)$$

The reason (38) makes sense is that each oriented 1-simplex connecting two adjacent points Ω and Ω' , defines the following isomorphism $\Sigma(\Omega) \rightarrow \Sigma(\Omega')$: we first reduce states in $\Sigma(\Omega)$ to $\Omega \cap \Omega'$ by elementary steps of restrictions, and then we extend the support of these states to Ω' by elementary steps of extensions. These steps are isomorphisms between information convex sets. After we apply these isomorphisms on $\vec{\gamma}$, in a sequence given by the orientation, we generate a unique automorphism (38).

- Triangles (2-simplex) are the places where the loop can deform ($\vec{\gamma} \rightarrow \vec{\gamma}'$) without affecting the automorphism. We illustrate the deformation as



where only part of the loops $\vec{\gamma}$ and $\vec{\gamma}'$ in the neighborhood of the triangle are shown. The fact that $\Phi(\vec{\gamma}) = \Phi(\vec{\gamma}')$ can be checked from (Definition 13) and the discussion below Eq. (38).

We therefore argue that $\pi_1(\mathfrak{m}(\Omega, N))$ is the information that determines the nontrivial classes of deformation of immersed region Ω back to itself in the background manifold N . Automorphisms of $\Sigma(\Omega)$ coming from smooth deformations can be different *only if* two closed loops $\vec{\gamma}$ and $\vec{\gamma}'$ (both pass Ω) represent two different elements of $\pi_1(\mathfrak{m}(\Omega, N))$. In particular, if the loop $\vec{\gamma}$ can shrink to a point on $\mathfrak{m}(\Omega, N)$, the associated automorphism $\Phi(\vec{\gamma})$ must be the (trivial) identity map.

¹⁶We thank John McGreevy for this question.

B.1.2 Examples

We give a few simple examples to illustrate the immersion complex (Definition 13) and discuss its physical relevance. Recall

$$\mathfrak{M}(\omega, N) \equiv \coprod_{\Omega \in \mathcal{R}(\omega, N)} \mathfrak{m}(\Omega, N), \quad (40)$$

where $\mathcal{R}(\omega, N)$ is the set of representatives of immersed regions homeomorphic to ω , immersed in N . Our first example is about annuli immersed in a disk. Let ω be the annulus and $N = B^2$ be the disk.

$$\mathfrak{M}(\text{annulus}, B^2) = \coprod_{j=0}^{\infty} \mathfrak{m}(X(j), B^2), \quad (41)$$

where $X(j)$ for $j \geq 0$ represents an immersed annulus with turning number j . In particular, we can let $X(0) = X_8$ be the immersed “figure-8” and let $X(1) = X$ be the embedded annulus. We expect $\mathfrak{m}(X, B^2)$ to be simply connected and $\pi_1(\mathfrak{m}(X, B^2))$ is trivial.¹⁷ What is $\pi_1(\mathfrak{m}(X_8, B^2))$? From the intuition around Eq. (6), we conjecture that $\pi_1(\mathfrak{m}(X_8, B^2)) = \mathbb{Z}_2$. If this is true, the definition of anti-sector on X_8 , discussed near Eq. (6) is justified.

The second example is about annuli immersed in a sphere.

$$\mathfrak{M}(\text{annulus}, S^2) = \mathfrak{m}(X, S^2) \coprod \mathfrak{m}(X_8, S^2), \quad (42)$$

where X and X_8 are the only two classes of immersed annuli in the sphere (as discussed in Table 1). Thus $\mathfrak{M}(\text{annulus}, S^2)$ has two connected components. What are the fundamental groups π_1 of the connected components? $\pi_1(\mathfrak{m}(X, S^2))$ should contain \mathbb{Z}_2 as a quotient group. The related observation is that X can turn inside out on the sphere and the fact that such process can turn an anyon $a \in \mathcal{C}$ into anti-anyon $\bar{a} \in \mathcal{C}$, which is, in general, a different sector. (For a related discussion, see Appendix G of [14].) We conjecture that $\pi_1(\mathfrak{m}(X_8, S^2))$ is \mathbb{Z}_2 .

One simple example in 3-dimensional space is

$$\mathfrak{M}(\text{sphere shell}, B^3) = \mathfrak{m}(Z, B^3), \quad (43)$$

where Z , on the right-hand side, represents the embedded sphere shell in the 3-dimensional ball B^3 . Eq. (43) follows from the fact that there is a unique way to immerse a sphere S^2 in B^3 (or R^3), up to regular homotopy; this is an influential early result by Smale [38], which is also the topic of video [29]. It seems plausible that $\pi_1(\mathfrak{m}(Z, B^3)) = \mathbb{Z}_2$, but we do not know proofs. It is further interesting to consider

$$\mathfrak{M}(\text{genus-}g \text{ handlebodies}, B^3) = \mathfrak{m}(G_g, B^3), \quad (44)$$

where G_g is an embedded genus- g handlebody and g is a positive integer. As is indicated in Eq. (44), \mathfrak{M} is connected in this example. Genus- g handlebodies detect the “graph excitations” studied in [16, 17], where for $g = 1$ these graph excitations are flux loops. In general, $\pi_1(\mathfrak{m}(G_g, B^3))$ can have pretty nontrivial structure even though G_g are sectorizable regions.

Our last example is in 2D, where the background N is an annulus. Consider an annulus X embedded in an annulus $N = X_+$ that thickens X , as shown in Fig. 14. We ask

$$\pi_1(\mathfrak{m}(X, X_+)) = ? \quad (45)$$

Note that, $\pi_1(\mathfrak{m}(X, X_+))$ can be nontrivial even if $\mathfrak{m}(X, B^2)$ is trivial. Intuitively, in the process described in Fig. 14, a pair of twists are created locally and then transported around the annulus

¹⁷If we deform X back to itself, keeping the intermediate configurations embedded, the deformation must correspond to a loop in $\mathfrak{m}(X, B^2)$ that can shrink to a point. The argument is precisely that used to prove Lemma 4.3 of [14]. However, for the deformations allowing immersed intermediate configurations, the argument does not apply.

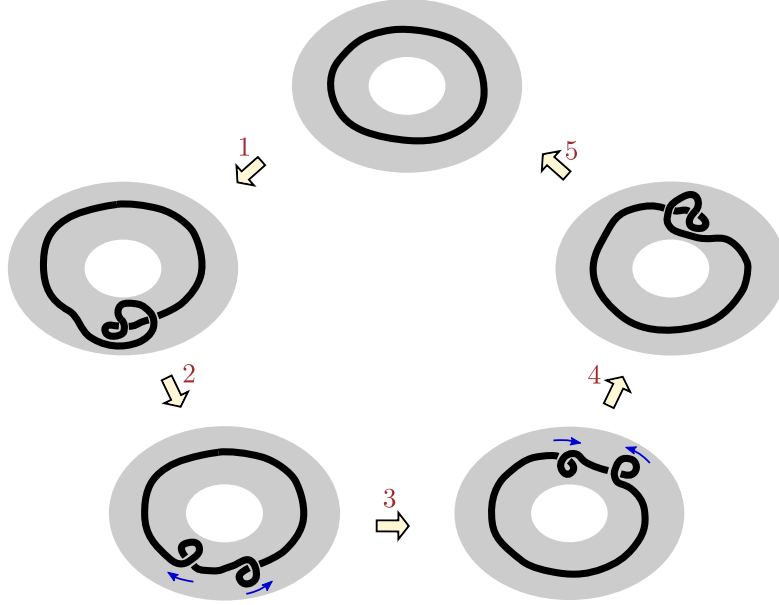


Figure 14: A deformation process, which corresponds to an oriented loop in $\mathfrak{m}(X, X_+)$. Here, X is an annulus (thick black loop in the top figure) embedded in a wider annulus X_+ (gray).

before they annihilate again. (The process in Fig. 14 is inspired by Fig. 8 of [39] as well as Fig. 7 of [20].) Can this process represent a nontrivial element of $\pi_1(\mathfrak{m}(X, X_+))$? We do not know the answer. If this process indeed corresponds to a non-contractible loop in $\mathfrak{m}(X, X_+)$, it may have nontrivial physical consequences in contexts with topological defects. Recall that references state on annulus X_+ may come from a system with a defect line that passes through X_+ as discussed in Section 5.

In summary, the problem we try to formulate in this section is meant to be a pure topology problem. This problem is carefully separated from the study of quantum states on such regions. Nonetheless, we believe this problem is a crucial mathematical problem towards a clear understanding of the automorphism of information convex sets. We wonder if the answers to these questions (or ones that are close analog) have appeared in math literature. The question on $\pi_0(\mathfrak{M}(\omega, N))$ is essentially the classification of immersion up to regular homotopy. Some related results can be looked up¹⁸ in existing math literature, e.g., [38, 39]. It is unclear to us if the fundamental group $\pi_1(\mathfrak{m}(\Omega, N))$, e.g., for examples listed above, has been studied in math literature. (That is why we only provided guesses to most answers!) In any case, entanglement bootstrap provides (adds) a motivation for the study of such mathematical objects.

B.2 Automorphisms utilizing tunneling

Tunneling trick (Section 3.1) provides extra isomorphism of information convex sets by “large changes” of the region, such as adding or removing a twist on a 1-handle. This is in contrast with the smooth deformation built from elementary steps. Tunneling is not described by lines in $\mathfrak{m}(\Omega, N)$. The tunneling trick, as described in the main text, works for the specific context of 2D. Below, we broaden the meaning of tunneling and use it to refer to any “large change” of an immersed region (together with the associated information convex set).

By allowing both smooth deformations and tunneling, we can obtain more diverse classes of automorphisms of $\Sigma(\Omega)$. We will not discuss the entire scope of how this might work, acknowledging

¹⁸Even in this case, we do not always find the results we want. We are most interested in manifolds with boundaries (such as punctured manifolds) immersed in a manifold with *the same* dimension. Sometimes, a math result we spent time searching for came out fresh [40].

that it is an interesting mathematical problem. Instead, we describe a nontrivial example in 2D.

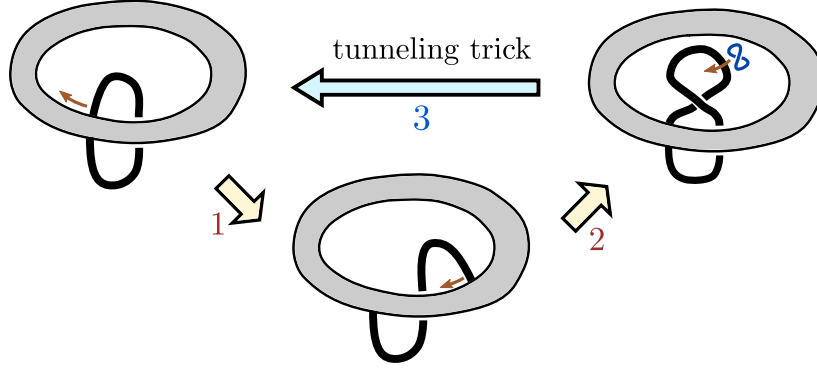


Figure 15: Automorphism of the information convex set of an immersed punctured torus, where tunneling is used. The punctured torus is visualized as an annulus (horizontal, gray) with a 1-handle (black) connecting both boundaries of the annulus.

Let \mathcal{W} be a punctured torus immersed in a disk B^2 , as shown in the left figure of Fig. 15. If there is an Abelian sector on figure-8 region, $\mu \in \mathcal{C}_8$, then we can design an automorphism of $\Sigma(\mathcal{W})$ utilizing the tunneling trick in one of the steps; see the process shown in Fig. 15. The entire process takes the immersed punctured torus \mathcal{W} back to itself. Steps 1 and 2 are smooth deformations.¹⁹ Step 3 is a tunneling. Thus, the automorphism cannot be associated with a closed loop in $\mathfrak{m}(\mathcal{W}, B^2)$. Is there any physical significance to this process? We anticipate that the answer is yes, relating this to the problem of defining topological spins from a state, but we postpone the discussion to future work.

C Strong isomorphism conjecture in arbitrary dimensions

Here is the statement of strong isomorphism conjecture for an arbitrary space dimension n , generalizing $n = 2$ case (Conjecture 6) in the main text. We denote the n -dimensional sphere on which we define the reference state as \mathbf{S}^n . Axioms **A0** and **A1** are satisfied everywhere.

Conjecture 14. *Suppose two immersed regions $\Omega, \Omega' \looparrowright \mathbf{S}^n$ are homeomorphic, then*

$$\Sigma(\Omega) \cong \Sigma(\Omega'). \quad (46)$$

Suppose this conjecture is true, then we have similar beliefs (as 2D, discussed in the discussion section) that the explicit isomorphisms that come up during the proof can be informative and useful in extracting universal information of the emergent topological quantum field theory associated with the reference state.

Besides, the strong isomorphism conjecture (Conjecture 14) seems to resonate with another basic question: “What is the definition of quantum dimension for an arbitrary immersed sectorizable region $S \looparrowright \mathbf{S}^n$?” This question is open for dimensions $n \geq 3$. Many (if not all) nontrivially immersed S have an embedded version $S^* \hookrightarrow \mathbf{S}^n$, where S^* is in the homeomorphism class of S . Since S^* is embedded, the quantum dimension of a superselection sector $I \in \mathcal{C}_{S^*}$ (characterized by $\Sigma(S^*)$) can be defined from the entropy difference of an extreme point ρ^I with the vacuum σ :

$$d_I \equiv \exp \left(\frac{S(\rho_{S^*}^I) - S(\sigma_{S^*})}{2} \right), \quad I \in \mathcal{C}_{S^*}. \quad (47)$$

¹⁹As a side note, I described steps 1 and 2 in a math student seminar in 2020 [41]; see the first backup slide, which was my attempt to ask about an unknown-to-me terminology. Later, my collaborators and I learned in the projects [16, 17] that the term I looked for was immersion and regular homotopy. Now step 3 is added, which gives a reason to ask more questions.

While Eq. (47) is familiar in early works, we are still interested in knowing if $d_I \geq 1$ in general. Nontrivial checks from 3D and gapped domain walls are consistent with $d_I \geq 1$, but the general proof for an arbitrary n is lacking. This puzzle can be restated as a question about the vacuum state: “Does the vacuum state have the absolute minimum entropy among states in $\Sigma(\Omega)$, for any $\Omega \hookrightarrow \mathbf{S}^n$?” We would like to conjecture the affirmative direction.

References

- [1] A. Kitaev and J. Preskill, “Topological entanglement entropy,” *Phys. Rev. Lett.* **96** (2006), no. 11 110404. [1](#)
- [2] M. Levin and X.-G. Wen, “Detecting topological order in a ground state wave function,” *Phys. Rev. Lett.* **96** (2006), no. 11 110405. [1](#), [18](#)
- [3] P. Calabrese and J. Cardy, “Entanglement entropy and conformal field theory,” *J. Phys. A* **42** (2009) 504005, [0905.4013](#). [1](#)
- [4] H. Li and F. D. M. Haldane, “Entanglement Spectrum as a Generalization of Entanglement Entropy: Identification of Topological Order in Non-Abelian Fractional Quantum Hall Effect States,” *Phys. Rev. Lett.* **101** (July, 2008) 010504, [0805.0332](#). [1](#)
- [5] I. Marvian, “Symmetry-Protected Topological Entanglement,” *arXiv e-prints* (July, 2013) arXiv:1307.6617, [1307.6617](#). [1](#)
- [6] H. Shapourian, K. Shiozaki, and S. Ryu, “Many-Body Topological Invariants for Fermionic Symmetry-Protected Topological Phases,” *Phys. Rev. Lett.* **118** (May, 2017) 216402, [1607.03896](#). [1](#)
- [7] Y. Zou, K. Siva, T. Soejima, R. S. K. Mong, and M. P. Zaletel, “Universal Tripartite Entanglement in One-Dimensional Many-Body Systems,” *Phys. Rev. Lett.* **126** (Mar., 2021) 120501, [2011.11864](#). [1](#)
- [8] I. H. Kim, B. Shi, K. Kato, and V. V. Albert, “Chiral Central Charge from a Single Bulk Wave Function,” *Phys. Rev. Lett.* **128** (Apr., 2022) 176402, [2110.06932](#). [1](#), [4](#)
- [9] R. Fan, R. Sahay, and A. Vishwanath, “Extracting the Quantum Hall Conductance from a Single Bulk Wave Function,” *Phys. Rev. Lett.* **131** (Nov., 2023) 186301, [2208.11710](#). [1](#)
- [10] Z.-P. Cian, M. Hafezi, and M. Barkeshli, “Extracting Wilson loop operators and fractional statistics from a single bulk ground state,” *arXiv e-prints* (Sept., 2022) arXiv:2209.14302, [2209.14302](#). [1](#)
- [11] T.-C. Lin and J. McGreevy, “Conformal Field Theory Ground States as Critical Points of an Entropy Function,” *Phys. Rev. Lett.* **131** (Dec., 2023) 251602, [2303.05444](#). [1](#)
- [12] I. H. Kim, “Long-Range Entanglement Is Necessary for a Topological Storage of Quantum Information,” *Phys. Rev. Lett.* **111** (Aug., 2013) 080503, [1304.3925](#). [1](#)
- [13] B. Shi, “Seeing topological entanglement through the information convex,” *Phys. Rev. Res.* **1** (Oct., 2019) 033048, [1810.01986](#). [1](#)
- [14] B. Shi, K. Kato, and I. H. Kim, “Fusion rules from entanglement,” *Annals of Physics* **418** (2020) 168164, [1906.09376](#). [1](#), [2](#), [4](#), [5](#), [11](#), [13](#), [18](#), [25](#)
- [15] B. Shi and I. H. Kim, “Entanglement bootstrap approach for gapped domain walls,” *Phys. Rev. B* **103** (2021), no. 11 115150, [2008.11793](#). [1](#), [6](#), [11](#)

- [16] J.-L. Huang, J. McGreevy, and B. Shi, “Knots and entanglement,” *SciPost Phys.* **14** (2023) 141, <https://scipost.org/10.21468/SciPostPhys.14.6.141>. 1, 2, 3, 4, 16, 22, 25, 27
- [17] B. Shi, J.-L. Huang, and J. McGreevy, “Remote detectability from entanglement bootstrap I: Kirby’s torus trick,” *arXiv e-prints* (Jan., 2023) arXiv:2301.07119, [2301.07119](https://arxiv.org/abs/2301.07119). 1, 2, 17, 18, 22, 25, 27
- [18] B. Shi, “Verlinde formula from entanglement,” *Phys. Rev. Res.* **2** (May, 2020) 023132, [1911.01470](https://arxiv.org/abs/1911.01470). 1
- [19] M. B. Hastings, “Classifying quantum phases with the Kirby torus trick,” *Phys. Rev. B* **88** (2013), no. 16 165114, [1305.6625](https://arxiv.org/abs/1305.6625). 2
- [20] M. Freedman and M. B. Hastings, “Classification of Quantum Cellular Automata,” *Comm. Math. Phys.* **376** (Apr., 2020) 1171–1222, [1902.10285](https://arxiv.org/abs/1902.10285). 2, 26
- [21] A. Kitaev, “On the Classification of Short-Range Entangled States,” *unpublished* (2013) <http://scgp.stonybrook.edu/archives/7874>. 2
- [22] E. H. Lieb and M. B. Ruskai, “Proof of the strong subadditivity of quantum mechanical entropy,” *J. Math. Phys.* **14** (1973), no. 12 1938–1941, <https://doi.org/10.1063/1.1666274>. 3
- [23] M. A. Levin and X.-G. Wen, “String-net condensation: A physical mechanism for topological phases,” *Phys. Rev. B* **71** (Jan., 2005) 045110, [cond-mat/0404617](https://arxiv.org/abs/cond-mat/0404617). 3, 18
- [24] R. Fan, P. Zhang, and Y. Gu, “Generalized real-space Chern number formula and entanglement hamiltonian,” *SciPost Physics* **15** (Dec., 2023) 249, [2211.04510](https://arxiv.org/abs/2211.04510). 4
- [25] N. Goldenfeld, “There’s Plenty of Room in the Middle: The Unsung Revolution of the Renormalization Group,” *arXiv e-prints* (June, 2023) arXiv:2306.06020, [2306.06020](https://arxiv.org/abs/2306.06020). 4
- [26] R. P. Feynman, “Plenty of Room at the Bottom,” in *APS annual meeting*, pp. 1–7, Little Brown Boston, MA, USA, 1959. 4
- [27] B. Shi, *Anyon theory in gapped many-body systems from entanglement*. PhD thesis, Ohio State University, 2020. 4
- [28] U. Pinkall, “Regular homotopy classes of immersed surfaces,” *Topology* **24** (1985), no. 4 421–434. 4, 24
- [29] S. Levy, D. Maxwell, and T. Munzner, “Outside In,” *AK Peters, Wellesley, MA* (1994) <https://www.youtube.com/watch?v=wO61D9x6lNY>. 5, 20, 25
- [30] D. Petz, “Monotonicity of Quantum Relative Entropy Revisited,” *Rev. Math. Phys.* **15** (2003) 79–91, [quant-ph/0209053](https://arxiv.org/abs/quant-ph/0209053). 10
- [31] K. Kato, F. Furrer, and M. Murao, “Information-theoretical analysis of topological entanglement entropy and multipartite correlations,” *Phys. Rev. A* **93** (Feb., 2016) 022317, [1505.01917](https://arxiv.org/abs/1505.01917). 11
- [32] R. E. Gompf and A. Stipsicz, *4-manifolds and Kirby calculus*. No. 20. American Mathematical Soc., 1999. 11
- [33] T. George, “The Classification of surfaces with Boundary,” *lecture notes*, (August 26, 2011) <https://www.math.uchicago.edu/~may/VIGRE/VIGRE2011/REUPapers/George.pdf>. 12

- [34] H. Bombin, “Topological Order with a Twist: Ising Anyons from an Abelian Model,” *Phys. Rev. Lett.* **105** (July, 2010) 030403, [1004.1838](#). [16](#)
- [35] M. Barkeshli, P. Bonderson, M. Cheng, and Z. Wang, “Symmetry Fractionalization, Defects, and Gauging of Topological Phases,” *arXiv e-prints* (Oct., 2014) arXiv:1410.4540, [1410.4540](#). [16](#)
- [36] B. Shi and Y.-M. Lu, “Characterizing topological order by the information convex,” *Phys. Rev. B* **99** (2019), no. 3 035112, [1801.01519](#). [16](#)
- [37] K. Kawagoe and M. Levin, “Microscopic definitions of anyon data,” *Phys. Rev. B.* **101** (Mar., 2020) 115113, [1910.11353](#). [19](#)
- [38] S. Smale, “A classification of immersions of the two-sphere,” *Transactions of the American Mathematical Society* **90** (1959), no. 2 281–290. [24](#), [25](#), [26](#)
- [39] J. Hass and J. Hughes, “Immersions of surfaces in 3-manifolds,” *Topology* **24** (1985), no. 1 97–112. [24](#), [26](#)
- [40] M. Freedman, D. Kasprowski, M. Kreck, A. W. Reid, and P. Teichner, “Immersions of punctured 4-manifolds,” *arXiv e-prints* (Aug., 2022) arXiv:2208.03064, [2208.03064](#). [26](#)
- [41] B. Shi, “Entanglement bootstrap: from gapped many-body ground states to emergent laws,” *Quantum Symmetries Student Seminar, Math-OSU* (2020) <https://bpb-us-w2.wpmucdn.com/u.osu.edu/dist/5/92910/files/2020/10/Entanglement-bootstrap-talk-Math-OSU.pdf>. [27](#)